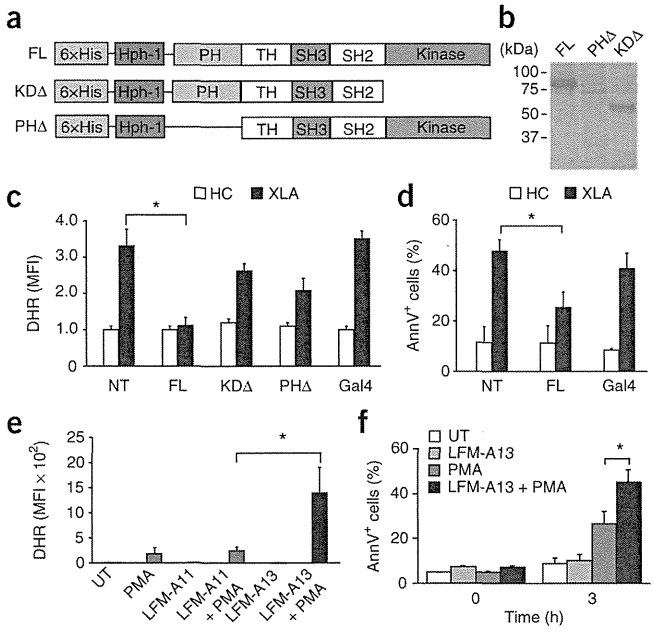

Figure 3 Excessive production of ROS and apoptosis in neutrophils from patients with XLA are abrogated by transduction of Hph-1–tagged full-length recombinant Btk but not by Hph-1–tagged Btk with deletion of the kinase or PH domain. (**a**) Hph-1–tagged Btk constructs: full-length Btk (FL); Btk with deletion of the kinase domain (KDΔ); Btk with deletion of the PH domain (PHΔ). 6×His, six-histidine tag; TH, Tec homology; SH3, Src homology 3; SH2, Src homology 2. (**b**) Size of purified Hph-1–tagged Btk proteins, confirmed by Coomassie brilliant blue staining. (**c**) ROS production in neutrophils from healthy controls ($n = 5$) and patients with XLA ($n = 5$), left untransduced (NT) or transduced with the constructs in **a** or Hph-1–tagged yeast transcriptional activator Gal4 (far right; control), presented as the MFI of DHR123 relative to that of untreated neutrophils from healthy controls, set as 1. (**d**) Frequency of apoptotic cells among neutrophils from healthy controls and patients with XLA, left untransduced or transduced with Hph-1–tagged full-length Btk or Gal4 (control). (**e**) DHR123 fluorescence in neutrophils from healthy controls ($n = 7$) left untreated or treated with PMA alone, or pretreated with LFM-A13 (Btk inhibitor) or LFM-A11 (control) alone or followed by stimulation with PMA (+ PMA). (**f**) Frequency of annexin V–positive cells among neutrophils from healthy controls ($n = 7$) left untreated or treated with PMA alone, or pretreated with LFM-A13 (50 μM, a concentration that does not inhibit other PTKs[47,48]) alone or followed by stimulation with PMA. $^*P = 0.0021$ (**c**), 0.019 (**d**), 0.021 (**e**) or 0.025 (**f**; Student's *t*-test). Data are representative of five experiments (**b**) or are pooled from six (**c**), three (**d**) or four (**e**,**f**) independent experiments (mean and s.d. in **c**–**f**).

signaling via TLRs or G protein–coupled receptors because of translocation to the plasma membrane[2]. Immunoblot analysis with antibody to gp91 (anti-gp91; **Fig. 4b**) and flow cytometry analysis of surface flavocytochrome b_{558} (**Fig. 4d**) showed higher gp91 expression in neutrophils from patients with XLA. Immunohistochemical analysis by confocal fluorescence microscopy showed localization of gp91 and Rac2 together in the membranes of resting Btk-deficient neutrophils but not in neutrophils from healthy controls (**Fig. 4e**). These results suggested that NADPH oxidase complex was partially assembled and ready to be activated in steady-state Btk-deficient neutrophils.

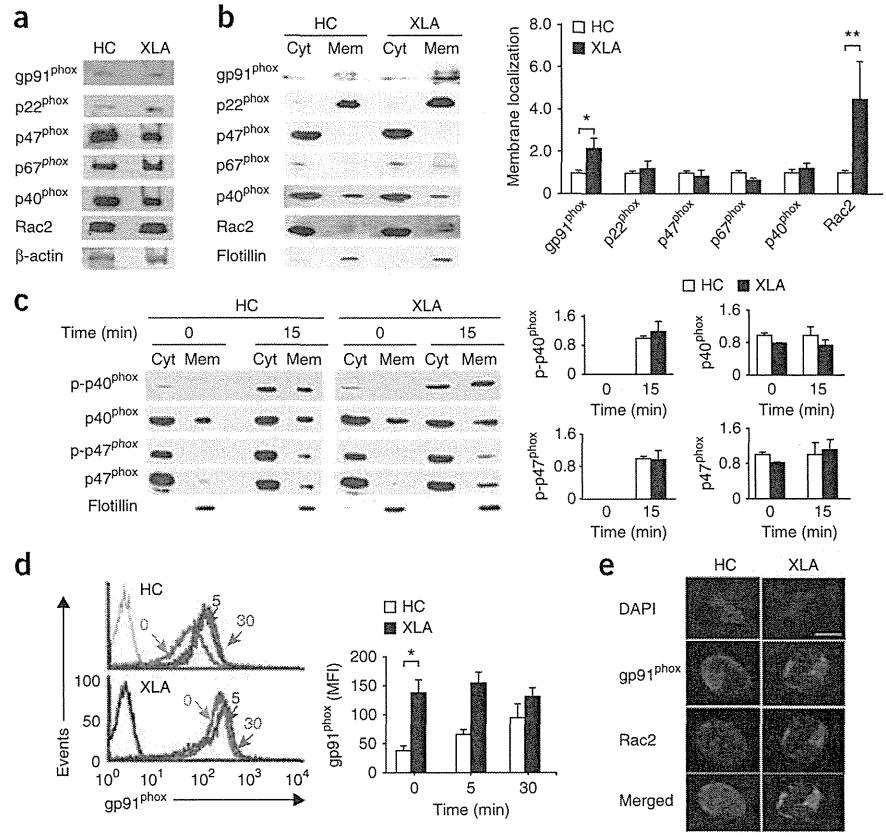

Figure 4 Btk-deficient neutrophils show targeting of Rac2 to the plasma membrane, colocalization of Rac2 with gp91^{phox} and higher membrane expression of gp91^{phox}. (**a**) Immunoblot analysis of the components of the NADPH oxidase complex in neutrophils from a healthy control and a patient with XLA. β-actin serves as a loading control throughout. (**b**) Immunoblot analysis (left) of the components of the NADPH oxidase complex in the cytoplasm (Cyt) and plasma membrane (Mem) of neutrophils from healthy controls and patients with XLA ($n = 9$ per group). Right, quantification of the membrane expression at left, presented as band intensity relative to that of flotillin (loading marker for the membrane-raft fraction) in membranes of neutrophils from healthy controls, set as 1. $^*P = 0.045$ and $^{**}P = 0.027$ (Student's *t*-test). (**c**) Immunoblot analysis of total and phosphorylated (p-) p40^{phox} and p47^{phox} in the cytoplasm and membrane of PMA-stimulated neutrophils from healthy controls and patients with XLA. Right, quantification as in **b**. (**d**) Flow cytometry analysis of gp91^{phox} on neutrophils from healthy controls and patients with XLA, left unstimulated (0) or stimulated for 5 or 30 min (above lines) with PMA, detected by staining with mAb 7D5 to gp91. Gray lines indicate staining with MsIgG (control). Right, quantification of the gp91 MFI in cells treated as at left. $^*P = 0.0039$ (Student's *t*-test). (**e**) Confocal microscopy of gp91^{phox} (green) and Rac2 (red) in healthy controls and neutrophils from patients with XLA; nuclei are counterstained with the DNA-intercalating dye DAPI (blue). Original magnification, ×600; scale bar, 10 μm. Data are from one representative of nine independent experiments with seven healthy controls and nine patients with XLA (**a**), are representative of nine experiments (**b**), are from nine independent experiments (**c**), are pooled from seven independent experiments (**d**) or are representative of four independent experiments (**e**; mean and s.d. in **b**–**d**).

Activated PTKs and PI(3)K in resting XLA neutrophils

Assembly and activation of the cytosolic components and Rac requires the involvement of kinases such as PTKs, PI(3)K and protein kinase C. We thus explored a potential signaling pathway that would lead to the partial assembly of NADPH oxidase. First, we examined the extent of tyrosine phosphorylation of cellular substrates in Btk-deficient and Btk-sufficient neutrophils before and after stimulation with PMA. Btk-deficient neutrophils showed hyperphosphorylation of protein species in the range of 50–53 kilodaltons (kDa), 72 kDa, 85 kDa and 150 kDa at baseline relative to phosphorylation in neutrophils from healthy controls (**Fig. 5a**). TLR4-mediated stimulation led to more phosphorylation of protein species 38 kDa, 50–53 kDa, 60 kDa, 72 kDa and 85 kDa in size in Btk-deficient neutrophils (**Supplementary Fig. 4a**).

In contrast, the baseline PTK activity in monocytes from patients with XLA was unaltered or slightly diminished relative to that of monocytes from healthy controls. TLR2-stimulated activation of PTKs was largely similar or slightly less in the absence of Btk (**Supplementary Fig. 4b**). We were able to directly ascribe the enhanced PTK activity to the absence of Btk, as transduction of recombinant Btk into neutrophils from patients with XLA restored baseline phosphorylation to that seen in neutrophils from healthy controls (**Fig. 5b**).

We next searched for tyrosine-phosphorylated proteins in Btk-deficient neutrophils through the use of phosphorylation-specific antibodies. The expression and activation of Tec and Bmx, TFKs present in neutrophils, was not upregulated in neutrophils from patients with XLA (**Fig. 5c**), which indicated that they did not compensate for Btk function. However, we found that the tyrosine-phosphorylated proteins 50–53 kDa, 72 kDa, 85 kDa and 150 kDa in size were the kinases Lyn and c-Src, Syk, the p85 subunit of PI(3)K (class IA) and FAK, respectively (**Fig. 5d,e**). We found that c-Src, Syk, PI(3)K-p85 and FAK were phosphorylated at their tyrosine residues that have a positive regulatory function. Notably, Lyn, a kinase known to have positive as well as negative roles in the modulation of myeloid function, was phosphorylated at Tyr507, a negative regulatory site[29–31].

We first focused on PI(3)K, as PI(3)K activation targets Rac2 to flavocytochrome b_{558}; this process is important for converting

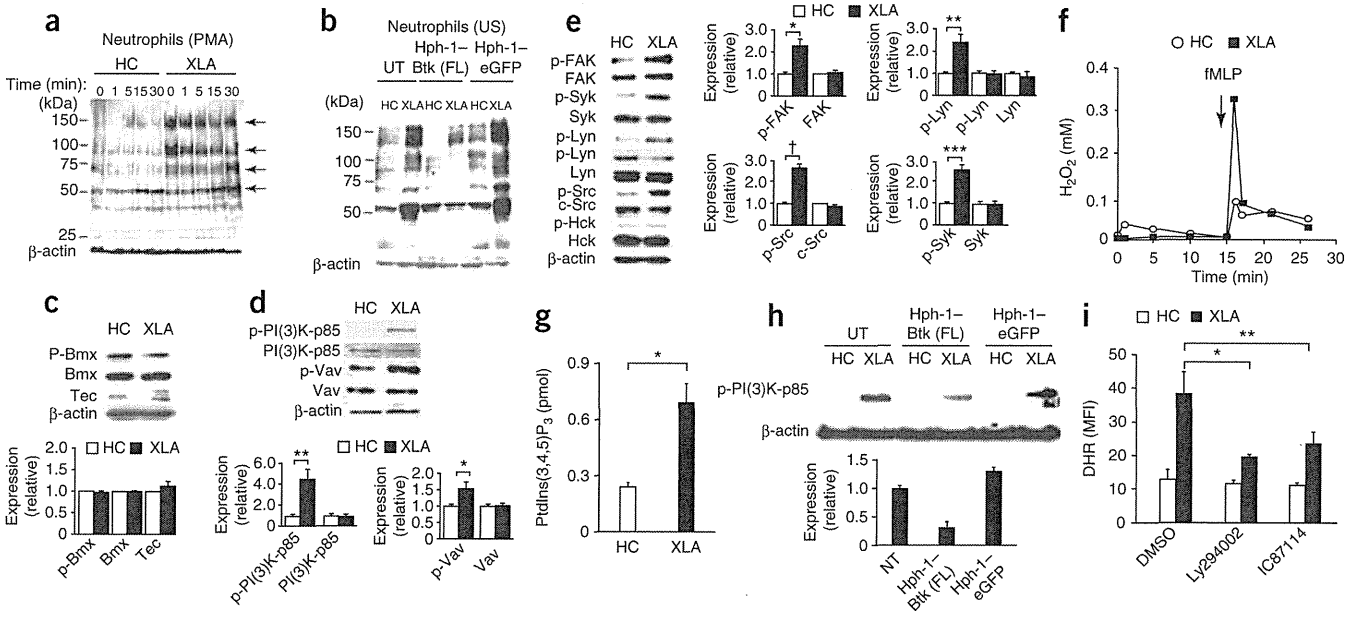

Figure 5 Btk-deficient neutrophils have higher baseline activity of PTKs and PI(3)K, which is reversed by transduction of recombinant Btk protein. (**a**) Immunoblot analysis of phosphorylated tyrosine in lysates of PMA-stimulated neutrophils from healthy controls ($n = 5$) and patients with XLA ($n = 7$). Arrows indicate hyperphosphorylated proteins in neutrophils from patients with XLA at 0 min. (**b**) Immunoblot analysis of phosphorylated tyrosine (as in **a**) in lysates from unstimulated (US) neutrophils from healthy controls ($n = 4$) and patients with XLA ($n = 5$), left untransduced or transduced with Hph-1-tagged full-length Btk or eGFP. (**c**,**d**) Immunoblot analysis (top) of whole-cell lysates of neutrophils from healthy controls ($n = 5$) and patients with XLA ($n = 7$), probed for total and phosphorylated Bmx and total Tec (**c**) or total and phosphorylated PI(3)K-p85 and Vav (phosphorylated at Tyr508 (PI(3)K-p85) or Tyr174 (Vav); **d**). Phosphorylated Tec was not detected by immunoblot analysis of phosphorylated tyrosine in samples immunoprecipitated with anti-Tec (data not shown). Bottom, quantification of the expression at top, presented relative to expression of β-actin in neutrophils from healthy controls, set as 1. $*P = 0.038$ and $**P = 0.0001$ (Student's *t*-test). (**e**) Immunoblot analysis (left) of neutrophils from healthy controls ($n = 5$) and patients with XLA ($n = 7$), probed for total PTKs and PTKs phosphorylated at Tyr576 and Tyr577 (FAK); Tyr524 and Tyr525 (Syk); Tyr507 (Lyn; top) or Tyr397 (Lyn; bottom); (Tyr416 (c-Src); and Tyr411 (the kinase Hck). Phosphorylated PTKs Fgr and Yes were undetectable (data not shown). Right, quantification as in **c**,**d**. $*P = 0.033$, $**P = 0.004$, $***P = 0.0007$ and $\dagger P = 0.0002$ (Student's *t*-test). (**f**) H_2O_2 production by fMLP-stimulated neutrophils from healthy controls and patients with XLA ($n = 5$ per group). (**g**) Enzyme-linked immunosorbent assay of phosphatidylinositol-(3,4,5)-trisphosphate (PtdIns(3,4,5)P_3) in unstimulated neutrophils from patients with XLA ($n = 5$). $*P = 0.0005$ (Student's *t*-test). (**h**) Immunoblot analysis (top) of phosphorylated PI(3)K-p85 in neutrophils from healthy controls and patients with XLA ($n = 5$ per group), left untransduced or transduced with Hph-1–tagged full-length Btk or eGFP. Detection of phosphorylated PI(3)K-p85 in neutrophils from healthy controls required longer exposure. Below, quantification of results above, presented relative to the expression of phosphorylated PI(3)K-p85 relative to that of β-actin in neutrophils from patients with XLA, set as 1. (**i**) Production of ROS in neutrophils from patients with XLA, treated with dimethyl sulfoxide (DMSO) or preincubated with Ly294002 (universal PI(3)K inhibitor; 50 μM)[32] or IC87114 (PI(3)Kδ inhibitor; 1 μM (a concentration that does not inhibit PI(3)Kα, PI(3)Kβ or PI(3)Kγ)[33]) and stimulated with fMLP. $*P = 0.006$ and $**P = 0.003$ (Student's *t*-test). Data are representative of or pooled from six (**a**,**f**), seven (**b**–**e**), four (**g**), eight (**h**) or five (**i**) independent experiments (mean and s.d. in **c**–**e**,**g**–**i**).

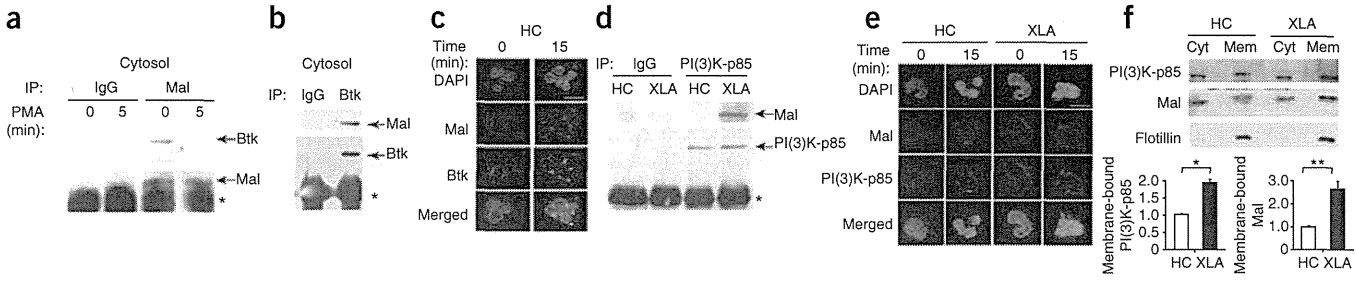

Figure 6 Mal in neutrophils from healthy controls associates with Btk in the resting state and translocates to the plasma membrane after stimulation, whereas Mal associates with PI(3)K at the plasma membrane in Btk-deficient neutrophils. (**a**,**b**) Coimmunoprecipitation analysis of Btk and Mal in the cytoplasmic fraction of neutrophils from healthy controls, left unstimulated (0 (**a**), **b**) or stimulated for 5 min with PMA (5 (**a**)). IP, immunoprecipitation; IgG, control antibody. *, immunoglobulin light chain (**a**) or heavy chain (**b**). (**c**) Confocal microscopy of neutrophils from healthy controls, left unstimulated (0) or stimulated for 15 min with PMA (15), then stained with anti-Mal (red) and anti-Btk (green) and counterstained with DAPI. Original magnification, ×600; scale bar, 10 μm. (**d**) Coprecipitation analysis of PI(3)K-p85 and Mal in membrane fraction of neutrophils from healthy controls and patients with XLA. *, immunoglobulin heavy chain. (**e**) Confocal microscopy of neutrophils from healthy controls and patients with XLA, left unstimulated or stimulated for 15 min with PMA, then stained with anti-Mal (red) and anti-PI(3)K-p85 (green) and counterstained with DAPI. Scale bar, 10 μm. (**f**) Immunoblot analysis (above) of PI(3)K-p85 and Mal in the cytoplasm and plasma membrane of unstimulated neutrophils from healthy controls and patients with XLA. Below, quantification of results above, presented relative to the expression of flotillin in neutrophils from healthy controls, set as 1. $*P = 0.0035$ and $**P = 0.0021$ (Student's *t*-test). Data are representative of three (**a**,**b**), four (**c**,**e**), six (**d**) or seven (**f**) independent experiments (mean and s.d. in **f**).

neutrophils into a 'primed' state in which they are ready for complete activation of NADPH oxidase triggered by stimuli such as fMLP. Indeed, Btk-deficient neutrophils were in a primed state, as fMLP alone elicited excessive production of ROS (**Fig. 5f**). Greater phosphorylation of PI(3)K-p85 was accompanied by more enzymatic activity, as shown by more baseline production of phosphatidylinositol-(3,4,5)-trisphosphate and by phosphorylation of the adaptor Vav (**Fig. 5d**,**g**). Furthermore, augmented PI(3)K activation was normalized, although only partially, by transduction of full-length Btk linked to Hph-1 (**Fig. 5h**).

The importance of PI(3)K in inducing the primed state was supported by data showing inhibition of fMLP-driven production of ROS by preincubation of Btk-deficient neutrophils with the universal PI(3)K inhibitor LY294002 at a concentration of 50 μM (refs. 32,33). We observed this inhibition in cells incubated with the PI(3)Kδ–specific inhibitor IC87114 at a concentration of 1 μM (ref. 33) but not in those incubated with the PI(3)Kγ–specific inhibitor AS605240 at a concentration of 8 nM (ref. 34; **Fig. 5i** and **Supplementary Fig. 5a**). These findings suggested PI(3)Kδ activation was involved in the excessive ROS response.

Interaction of membrane-targeted Mal with PI(3)K

We next sought the reason for the PI(3)K activation in the absence of Btk. For this, we first focused on a molecule that interacts with both Btk and PI(3)K. Evidence obtained with monocytes indicates that Mal is a critical component of TLR2-TLR4 signaling and is a target of Btk[13,14,20,21]. The TLR signal triggers activation of Btk, which in turn phosphorylates Mal. Phosphorylated Mal translocates to the plasma membrane via phosphatidylinositol-(4,5)-bisphosphate ($PtdIns(4,5)P_2$) and then interacts with and activates PI(3)K[35].

Unexpectedly, coimmunoprecipitation assays of neutrophils from human controls demonstrated that Mal was associated with Btk in the resting state (**Fig. 6a**,**b**). We observed colocalization of Mal and Btk in the cytoplasm and, after activation of cells with PMA, we detected the Mal-Btk complex at the membrane by immunofluorescence staining (**Fig. 6c**).

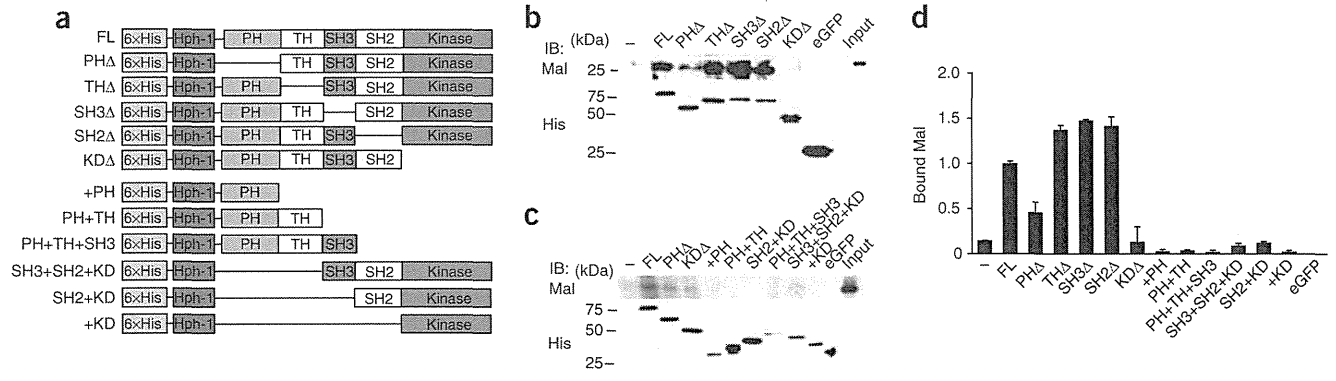

Figure 7 Btk associates with Mal at the PH and kinase domains. (**a**) Hph-1–tagged Btk constructs: full-length Btk (FL); Btk mutants with deletion of the PH domain (PHΔ), Tec homology (THΔ), SH3 domain (SH3Δ), SH2 domain (SH2Δ) or kinase domain (KDΔ); and Btk mutants with truncation retaining (+) only some domains (bottom six). (**b**,**c**) Immunoblot analysis (IB) of Mal (top) in extracts of cytoplasm of neutrophils from healthy controls, incubated with nickel beads bound to Hph-1–tagged recombinant full-length Btk or the deletion mutants (**b**) or truncation mutants (**c**) in **a**, or to Hph-1–tagged eGFP (negative control). Below, immunoblot analysis after rebinding to nickel beads, probed with anti-histidine (His). To make these as equimolar as possible, more beads were added for the +PH, PH+TH+SH3, SH3+SH2+KD and +KD constructs. Input, cytoplasmic extracts without precipitation. (**d**) Quantification of Mal bound to the recombinant Btk proteins based on the results in **b**,**c** ($n = 4$ donors), presented to results for full-length Btk, set as 1. Data are representative of four experiments (**b**,**c**) or are a summary of four independent experiments (**d**; mean and s.d.).

We did not detect the association of Mal with PI(3)K-p85 in unstimulated neutrophils from healthy controls; however, we did observe this association in Btk-deficient neutrophils before stimulation with PMA (**Fig. 6d**). Moreover, confocal fluorescence microscopy showed targeting of the PI(3)K-p85–Mal complex to the membrane in the absence of Btk, whereas we observed the complex at the membrane after stimulation with PMA in the presence of Btk (**Fig. 6e**). In addition, most of the PI(3)K-p85 and Mal was present in the membrane fraction in neutrophils from patients with XLA (**Fig. 6f**). These data suggested that Btk in resting neutrophils was involved in confining Mal to the cytoplasm.

The mode of the Btk-Mal association

Btk phosphorylates Mal at Tyr86, Tyr106 and Tyr187, and the Btk-Mal interaction requires Pro125, Tyr86, Tyr106 and Tyr159 in Mal, whereas the critical site in Btk for this association remains unknown[21,22]. To clarify the region of Btk required for the cytoplasmic Btk-Mal association, we generated various Btk deletion mutants fused to histidine-tagged Hph-1 (**Fig. 7a**) and assessed their binding to Mal (**Fig. 7**). We incubated nickel bead–bound recombinant proteins with the cytoplasmic fraction of control neutrophils and evaluated the associations by immunoblot analysis with anti-Mal. Full-length Btk effectively bound to cytoplasmic Mal prepared from control neutrophils, but a control fusion of histidine-tagged Hph-1 and enhanced green fluorescent protein (eGFP) did not. Btk with deletion of the kinase domain almost completely lost the ability to interact with Mal, and Btk with deletion of the PH domain showed less binding to Mal. In contrast, recombinant proteins lacking the Tec homology domain, the Src homology 3 domain or the Src homology 2 domain had slightly greater capacity to associate with Mal (**Fig. 7b,d**). Other truncated Btk recombinant proteins without either the PH domain or kinase domain failed to bind to Mal (**Fig. 7c,d**), which suggested that both the PH domain and kinase domain are critical for the Btk-Mal interaction.

PTKs associate with Mal and regulate PI(3)K activation

The precise mechanism of PI(3)K activation triggered by membrane-associated Mal is largely unknown. As several PTKs were phosphorylated

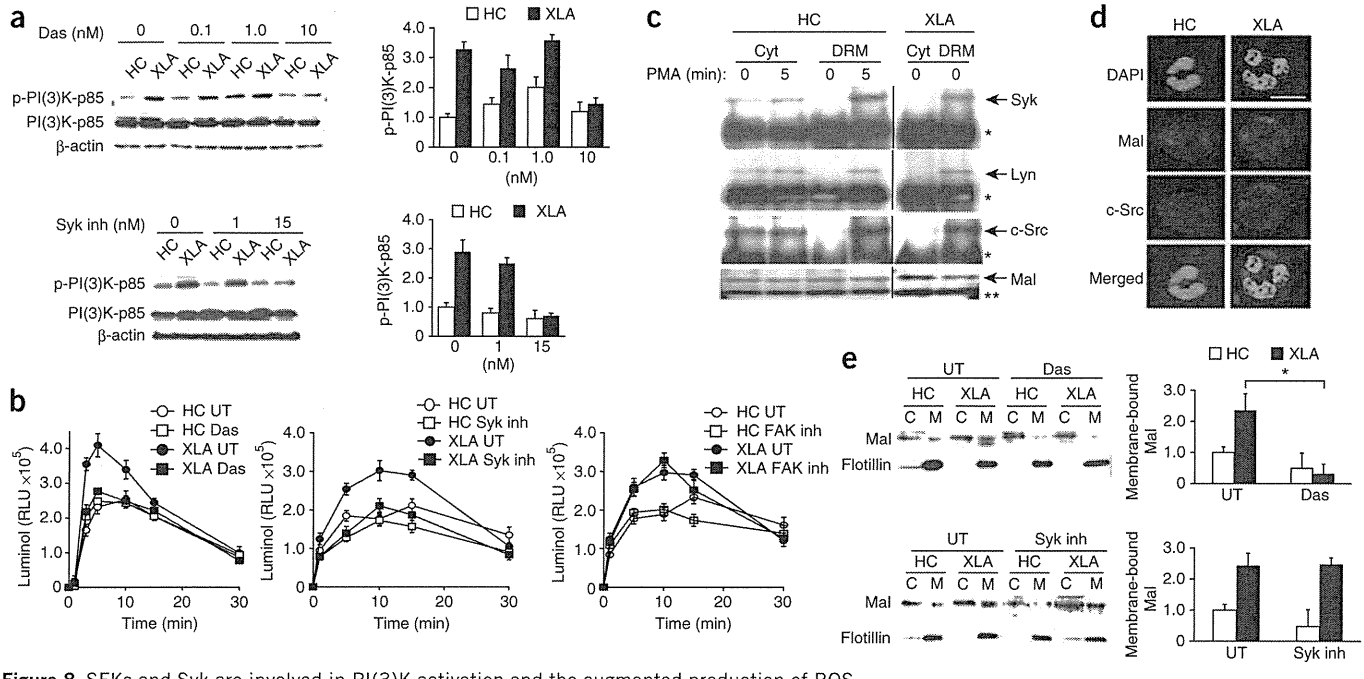

Figure 8 SFKs and Syk are involved in PI(3)K activation and the augmented production of ROS, whereas SFKs are involved in the membrane localization of Mal, in Btk-deficient neutrophils. (**a**) Immunoblot analysis (left of each pair) of total and phosphorylated PI(3)K-p85 in neutrophils from healthy controls and patients with XLA ($n = 4$ per group), treated with dasatinib (Das; at 10 nM, to inhibit the activity of c-Src, Lyn and Bcr-Abl but not FAK or Syk directly[36]) or a Syk inhibitor (Syk inh). Right (of each pair), densitometry of PI(3)K-p85 phosphorylated at Tyr508, presented as band intensity relative to that in untreated neutrophils from healthy controls, set as 1. (**b**) H_2O_2 production in neutrophils ($n = 4$ donors per group) left untreated (UT) or pretreated with dasatinib (10 nM), Syk inhibitor (15 nM) or FAK inhibitor (4 nM), and then stimulated with PMA, assessed by luminol assay and presented in relative light units (RLU). (**c**) Immunoassay of cytosolic fractions (Cyt) and detergent-resistant membrane fractions (DRM) of neutrophils from healthy controls and patients with XLA, left untreated (0) or treated for 5 min with PMA (5), followed by immunoprecipitation with anti-Mal and immunoblot analysis with anti-Syk, anti-Lyn, anti-c-Src or anti-Mal. *, immunoglobulin heavy chain; **, immunoglobulin light chain. (**d**) Confocal microscopy of neutrophils from healthy controls and patients with XLA ($n = 3$ per group), stained with anti-Mal (red) and anti-c-Src (blue) and counterstained with DAPI. Original magnification, ×600; scale bar, 10 μm. (**e**) Immunoblot analysis (left) of Mal in the cytoplasm (C) and membrane (M) of neutrophils from healthy controls and patients with XLA ($n = 5$ per group), left untreated or treated as in **a**. Right, quantification of results for Mal (left), presented relative to that of flotillin in the membrane fraction of neutrophils from healthy controls, set as 1. *$P = 0.0024$ (Student's t-test). (**f**) Immunoblot analysis of total Syk and Syk phosphorylated at Tyr524 and Tyr525 (top left) and of total c-Src and c-Src phosphorylated at Tyr416 (bottom left) in neutrophils from healthy controls and patients with XLA, left untreated or treated with dasatinib (top left) or Syk inhibitor (bottom left). Right, quantification of band intensity relative to that of β-actin in untreated neutrophils from healthy controls, set as 1. *$P = 0.013$ (Student's t-test). Data are from four (**a**) or five (**f**) independent experiments, are from one representative of four independent experiments (**c**) or are representative of four experiments (**b**,**e**) or three experiments (**c**; mean and s.d. in **a**,**b**,**e**,**f**).

in resting neutrophils from patients with XLA, we first used PTK inhibitors to investigate whether PTKs were involved in the PI(3)K activation. Inhibition of the activity of Src-family kinases (SFKs) by dasatinib (at a concentration of 10 nM)[36] led to normalized phosphorylation of PI(3)K-p85 in neutrophils derived from patients with XLA. Similarly, a Syk inhibitor (at a concentration of 15 nM)[37] but not a FAK inhibitor (at a concentration of 10 nM)[38] abrogated the hyperphosphorylation of PI(3)K (**Fig. 8a** and data not shown). The lower PI(3)K phosphorylation produced by dasatinib or the Syk inhibitor was accompanied by normalized production of ROS (**Fig. 8b**), which indicated that SFKs and Syk were involved in the augmented production of ROS in neutrophils from patients with XLA.

The findings noted above prompted us to determine whether the activated PTKs associated with Mal. SFKs are recruited to lipid rafts when activated for the assembly of signal components[39,40]. Coprecipitation assays showed that Lyn, c-Src and Syk interacted with Mal at the rafts of Btk-deficient neutrophils before stimulation (**Fig. 8c**). We also observed the colocalization of Mal and c-Src at the membrane by confocal fluorescence microscopy (**Fig. 8d**). We observed the interaction at the rafts of control neutrophils only after stimulation with PMA (**Fig. 8c** and **Supplementary Fig. 6**).

SFKs are cytoplasmic kinases and are anchored to the plasma membrane through myristoylation and palmitoylation[39,40]. Coprecipitation assays showed that Lyn, c-Src and Syk were associated with Mal in the cytosol of neutrophils from healthy controls but not in Btk-deficient neutrophils (**Fig. 8c**). We also confirmed by immunofluorescence staining the presence of c-Src associated with Mal in the cytoplasm but not in the membrane of normal resting neutrophils (**Fig. 8d**).

We next studied whether the membrane localization of Mal was regulated by SFKs or by Syk. The localization of Mal to the membrane in Btk-deficient neutrophils was diminished to normal amounts in cells treated with dasatinib but not those treated with the Syk inhibitor (**Fig. 8e**), which suggested that kinase activity of SFKs was required for membrane recruitment or maintenance of membrane-anchoring of Mal. Treatment of neutrophils from patients with XLA with dasatinib resulted in less baseline Syk phosphorylation, whereas incubation with the Syk inhibitor did not abrogate the hyperphosphorylation of c-Src (**Fig. 8f**), which indicated that Syk was downstream of SFKs in the steady-state signaling cascade of Btk-deficient neutrophils.

Collectively, the data reported above indicated that at least some PTKs associated with Mal together with Btk in the cytoplasm; in the absence of Btk, SFKs and Mal translocated to the membrane. The membrane-recruited PTKs formed a complex with and phosphorylated PI(3)K-p85 (**Supplementary Fig. 7**). It is still unclear which neutrophil SFK contributes to PI(3)K activation. Our findings may indicate that c-Src (or other SFKs) but not Lyn is (are) directly involved in the PI(3)K activation in Btk-deficient neutrophils; however, the possibility of an indirect contribution of Lyn to the phosphorylation of PI(3)K-p85 cannot be excluded solely by the inhibitor assay.

DISCUSSION

So far, most data have posited Btk as an essential molecule in innate immune responses[12–15,23,25]. Here we have shown that Btk is a negative regulator of signal transduction that leads to activation of NADPH oxidase and a molecule that prevents excessive neutrophil responses. Neutropenia in patients with XLA is usually induced by infection and is observed less often after immunoglobulin supplementation. This phenomenon can most probably be explained by ROS-mediated apoptosis of neutrophils triggered by the engagement of innate receptors and not by abnormal myeloid differentiation.

Our study suggested that Btk serves as a cytosolic component that interacts with Mal to prevent its translocation to the membrane and its interactions with PI(3)K until the appropriate stimulation is received. Both the PH and kinase domains of Btk were necessary for association with cytoplasmic Mal and were important for proper and coordinated initiation of the TLR and TNF receptor responses in human neutrophils. A similar mode of interaction has been demonstrated for the association of Btk with the cell-surface death receptor Fas (CD95) in B cells. Btk associates with Fas via its PH and kinase domains and prevents the interaction of Fas with the Fas-associated death domain and thus serves as a negative regulator of the Fas death-inducing signaling complex[41]. Notably, Btk serves as a negative regulator of apoptosis in both signaling systems.

SFKs were also involved in the baseline activation of PI(3)K in Btk-deficient neutrophils. We detected the association of c-Src, Lyn and Syk with Mal in the membrane raft in the absence of Btk. In addition, localization of Mal to the membrane in Btk-defective neutrophils was dependent on SFKs. These findings may indicate that SFKs serve as a substitute for the function of Btk in guiding the localization of Mal, albeit in an unregulated way. In neutrophils from control subjects, SFKs and Mal were associated in the cytoplasm and localized to the raft after stimulation. The mode of the SFK-Mal interaction remains unclear; however, we speculate that the kinase domain is involved, as SFKs lack a PH domain and the kinase domains of SFKs and Btk share 40–45% homology. Precise mapping of the Mal-binding site in the Btk kinase domain would help to clarify the SFK-Mal association site. Notably, neutrophils had more abundant expression of Mal than did monocytes (data not shown). Our data suggest that Mal is a critical coordinator of the priming signal and that its localization is tightly controlled by Btk.

Limited data indicate a role for PTKs in the production of ROS in neutrophils, particularly in humans. Lyn is reported to be a signaling component of the immunoglobulin receptors FcγRI and FcγRII or the receptor for the hematopoietic cytokine G-CSF, as well as an activator of PI(3)K[30,42], but is also noted for its ability to negatively regulate myeloid-cell signaling through phosphorylation of inhibitory receptors and recruitment of phosphatases[29]. Lyn-deficient neutrophils produce less ROS than Lyn-sufficient neutrophils do after stimulation with G-CSF[30] but show an enhanced respiratory burst after integrin-mediated signaling[29,31]. ROS responses triggered by *Aspergillus* species are totally dependent on Syk in mouse neutrophils[43]. The phosphorylation at different regulatory sites in Lyn versus c-Src in Btk-deficient neutrophils is notable. However, overall, PTKs in unstimulated neutrophils from patients with XLA seem to function as positive signal regulators. These data, along with our observations, suggest a potential contribution of SFKs and Syk to the early phase of NADPH oxidase activation in human neutrophils.

Activation of TFKs occurs downstream of SFKs in signaling pathways[40]. However, in neutrophils, Btk regulates baseline SFK activation. There are several possible mechanisms to explain how defective Btk is connected to SFK activation. We first speculated that Btk controls SFKs through the activation of negative SFK regulators. We investigated the Src kinase Csk and its regulatory molecule Cbp[44], but found no difference in the expression, localization or phosphorylation of Csk or Cbp (data not shown). As a second possible mechanism, SFKs but not TFKs may have been activated to compensate for Btk function in neutrophils. It is noteworthy that Btk regulates PtdIns(4,5)P_2 synthesis, acting as a shuttle to bring type I phosphatidylinositol-4-phosphate 5-kinases to the plasma membrane in B cells[45]. Although the role of Btk in PtdIns(4,5)P_2 production in human neutrophils has not been addressed, the generation of PtdIns(4,5)P_2 is a critical

step in the activation of NADPH oxidase. SFKs may have directly or indirectly served as a substitute for the function of Btk in neutrophils from patients with XLA. Finally, the cytoplasmic association of SFKs with Mal but without Btk may have resulted in SFK activation and Lyn inhibition. The phosphorylation of SFKs and subsequent modification of Mal by SFKs may have led to the translocation of Mal in the absence of Btk.

Neutrophils from patients with XLA show excessive production of ROS, but neutrophils from mice with X-linked immunodeficiency show poor ROS induction[15]. One possibility that could explain this discrepancy is the difference between mice and humans in the involvement of Btk in the NADPH oxidase pathway. Another possibility is the difference in the contributions of various members of the PI(3)K family to neutrophil activation. The primed production of ROS requires sequential activation of PI(3)Kγ and PI(3)Kδ in humans, whereas the production of ROS is largely dependent on PI(3)Kγ alone in mice[46]. A third possibility is differences in the methods of neutrophil collection from mice and in our study. Neutrophils collected from the peritoneum after treatment with thioglycolate broth may have been stimulated by that treatment[15]. The production of ROS was not augmented or compromised in neutrophils from patients with XLA in one study[26]. That may also have resulted from a relatively harsh isolation technique of hypotonic shock or from non–endotoxin-free conditions (for example, lipopolysaccharide in FBS) at any point of the experiment.

In this study, we have reported that Btk serves as a critical gatekeeper of neutrophil response. Our study suggests that the regulation of neutrophil activation and apoptosis in various human diseases could be achieved by manipulation of Btk. Future studies should explore the role of Btk in controlling the production of ROS and apoptosis of basophils, mast cells and eosinophils. Finally, ROS-mediated induction of apoptosis after suboptimal or optimal stimuli may be worth investigating in immature and precursor cells of the immune reponse to determine the role of Btk in their survival, proliferation and differentiation.

METHODS

Methods and any associated references are available in the online version of the paper at http://www.nature.com/natureimmunology/.

Note: Supplementary information is available on the Nature Immunology website.

ACKNOWLEDGMENTS

We thank E. Tsitsikov, E. Rachlin, K. Imai and J. Yata for discussions; all patients who participated in this study; S. Goo Rhee (Ewha Womans University) for antibody to Prx1 phosphorylated at Tyr194; and J.A. Lindquist (Otto-von-Guericke University) for antibody to Cbp (PAG) phosphorylated at Tyr317. Supported by the Ministry of Health, Labour and Welfare of Japan (H. Kane, S.N. and T.M.), the Ministry of Education, Culture, Sports, Science and Technology of Japan (S.M. and T.M.) and by the National Research Foundation of Korea (National Creative Research Initiatives grant to S.-K.L.).

AUTHOR CONTRIBUTIONS

F.H. did experiments; E.-S.K. and S.-K.L. contributed to protein-delivery experiments and provided some technical support; H. Kano and H. Kane made suggestions on data analysis and interpretation; S.N. and S.M. provided advice on project planning and data interpretation; M.T. provided advice on project plan and edited the manuscript; T.M. directed the project, designed research and wrote the manuscript; and all authors reviewed and approved the manuscript.

COMPETING FINANCIAL INTERESTS

The authors declare no competing financial interests.

Published online at http://www.nature.com/natureimmunology/.
Reprints and permissions information is available online at http://www.nature.com/reprints/index.html.

1. Flannagan, R.S., Cosio, G. & Grinstein, S. Antimicrobial mechanisms of phagocytes and bacterial evasion strategies. *Nat. Rev. Microbiol.* **7**, 355–366 (2009).
2. Nauseef, W.M. How human neutrophils kill and degrade microbes: an integrated view. *Immunol. Rev.* **219**, 88–102 (2007).
3. Lambeth, J.D. NOX enzymes and the biology of reactive oxygen. *Nat. Rev. Immunol.* **4**, 181–189 (2004).
4. Babior, B.M. NADPH oxidase. *Curr. Opin. Immunol.* **16**, 42–47 (2004).
5. Sumimoto, H. Structure, regulation and evolution of Nox-family NADPH oxidases that produce reactive oxygen species. *FEBS J.* **275**, 3249–3277 (2008).
6. Fang, F.C. Antimicrobial reactive oxygen and nitrogen species: concepts and controversies. *Nat. Rev. Microbiol.* **2**, 820–832 (2004).
7. Singh, A., Zarember, K.A., Kuhns, D.B. & Gallin, J.I. Impaired priming and activation of the neutrophil NADPH oxidase in patients with IRAK4 or NEMO deficiency. *J. Immunol.* **182**, 6410–6417 (2009).
8. Woollard, K.J. & Geissmann, F. Monocytes in atherosclerosis: subsets and functions. *Nat. Rev. Cardiol.* **7**, 77–86 (2009).
9. Finkel, T. Radical medicine: treating ageing to cure disease. *Nat. Rev. Mol. Cell Biol.* **6**, 971–976 (2005).
10. Conley, M.E. *et al.* Genetic analysis of patients with defects in early B-cell development. *Immunol. Rev.* **203**, 216–234 (2005).
11. Winkelstein, J.A. *et al.* X-linked agammaglobulinemia: report on a United States registry of 201 patients. *Medicine (Baltimore)* **85**, 193–202 (2006).
12. Mohamed, A.J. *et al.* Bruton's tyrosine kinase (Btk): function, regulation, and transformation with special emphasis on the PH domain. *Immunol. Rev.* **228**, 58–73 (2009).
13. Gray, P. *et al.* MyD88 adapter-like (Mal) is phosphorylated by Bruton's tyrosine kinase during TLR2 and TLR4 signal transduction. *J. Biol. Chem.* **281**, 10489–10495 (2006).
14. Doyle, S.L., Jefferies, C.A., Feighery, C. & O'Neill, L.A. Signaling by Toll-like receptors 8 and 9 requires Bruton's tyrosine kinase. *J. Biol. Chem.* **282**, 36953–36960 (2007).
15. Mangla, A. *et al.* Pleiotropic consequences of Bruton tyrosine kinase deficiency in myeloid lineages lead to poor inflammatory responses. *Blood* **104**, 1191–1197 (2004).
16. Fiedler, K. *et al.* Neutrophil development and function critically depend on Bruton tyrosine kinase in a mouse model of X-linked agammaglobulinemia. *Blood* **117**, 1329–1339 (2011).
17. Conley, M.E. *et al.* Primary B cell immunodeficiencies: comparisons and contrasts. *Annu. Rev. Immunol.* **27**, 199–227 (2009).
18. Kerner, J.D. *et al.* Impaired expansion of mouse B cell progenitors lacking Btk. *Immunity* **3**, 301–312 (1995).
19. Khan, W.N. *et al.* Defective B cell development and function in Btk-deficient mice. *Immunity* **3**, 283–299 (1995).
20. O'Neill, L.A.J. & Bowie, A.G. The family of five: TIR-domain-containing adaptors in Toll-like receptor signalling. *Nat. Rev. Immunol.* **7**, 353–364 (2007).
21. Piao, W. *et al.* Tyrosine phosphorylation of MyD88 adapter-like (Mal) is critical for signal transduction and blocked in endotoxin tolerance. *J. Biol. Chem.* **283**, 3109–3119 (2008).
22. Jenkins, K.A. & Mansell, A. TIR-containing adaptors in Toll-like receptor signalling. *Cytokine* **49**, 237–244 (2010).
23. Taneichi, H. *et al.* Toll-like receptor signaling is impaired in dendritic cells from patients with X-linked agammaglobulinemia. *Clin. Immunol.* **126**, 148–154 (2008).
24. Pérez de Diego, R. *et al.* Bruton's tyrosine kinase is not essential for LPS-induced activation of human monocytes. *J. Allergy Clin. Immunol.* **117**, 1462–1469 (2006).
25. Horwood, N.J. *et al.* Bruton's tyrosine kinase is required for TLR2 and TLR4-induced TNF, but not IL-6, production. *J. Immunol.* **176**, 3635–3641 (2006).
26. Marron, T.U., Rohr, K., Martinez-Gallo, M., Yu, J. & Cunningham-Rundles, C. TLR signaling and effector functions are intact in XLA neutrophils. *Clin. Immunol.* **137**, 74–80 (2010).
27. Honda, F. *et al.* Transducible form of p47phox and p67phox compensate for defective NADPH oxidase activity in neutrophils of patients with chronic granulomatous disease. *Biochem. Biophys. Res. Commun.* **417**, 162–168 (2012).
28. Dang, P.M. *et al.* A specific p47phox -serine phosphorylated by convergent MAPKs mediates neutrophil NADPH oxidase priming at inflammatory sites. *J. Clin. Invest.* **116**, 2033–2043 (2006).
29. Scapini, P., Pereira, S., Zhang, H. & Lowell, C.A. Multiple roles of Lyn kinase in myeloid cell signaling and function. *Immunol. Rev.* **228**, 23–40 (2009).
30. Zhu, Q.S. *et al.* G-CSF induced reactive oxygen species involves Lyn-PI3-kinase-Akt and contributes to myeloid cell growth. *Blood* **107**, 1847–1856 (2006).
31. Pereira, S. & Lowell, C. The Lyn tyrosine kinase negatively regulates neutrophil integrin signaling. *J. Immunol.* **171**, 1319–1327 (2003).
32. Vlahos, C.J., Matter, W.F., Hui, K.Y. & Brown, R.F. A specific inhibitor of phosphatidylinositol 3-kinase, 2-(4-morpholinyl)-8-phenyl-4H-1-benzopyran-4-one (LY294002). *J. Biol. Chem.* **269**, 5241–5248 (1994).
33. Sadhu, C., Masinovsky, B., Dick, K., Sowell, C.G. & Staunton, D.E. Essential role of phosphoinositide 3-kinase δ in neutrophil directional movement. *J. Immunol.* **170**, 2647–2654 (2003).
34. Morris, A.C. *et al.* C5a-mediated neutrophil dysfunction is RhoA-dependent and predicts infection in critically ill patients. *Blood* **117**, 5178–5188 (2011).
35. Santos-Sierra, S. *et al.* Mal connects TLR2 to PI3Kinase activation and phagocyte polarization. *EMBO J.* **28**, 2018–2027 (2009).

36. Nam, S. *et al.* Action of the Src family kinase inhibitor, dasatinib (BMS-354825), on human prostate cancer cells. *Cancer Res.* **65**, 9185–9189 (2005).
37. Lai, J.Y. *et al.* Potent small molecule inhibitors of spleen tyrosine kinase (Syk). *Bioorg. Med. Chem. Lett.* **13**, 3111–3114 (2003).
38. Slack-Davis, J.K. *et al.* Cellular characterization of a novel focal adhesion kinase inhibitor. *J. Biol. Chem.* **282**, 14845–14852 (2007).
39. Korade-Mirnics, Z. & Corey, S.J. Src kinase-mediated signaling in leukocytes. *J. Leukoc. Biol.* **68**, 603–613 (2000).
40. Bradshaw, J.M. The Src, Syk, and Tec family kinases: distinct types of molecular switches. *Cell. Signal.* **22**, 1175–1184 (2010).
41. Vassilev, A., Ozer, Z., Navara, C., Mahajan, S. & Uckun, F.M. Bruton's tyrosine kinase as an inhibitor of the Fas/CD95 death-inducing signaling complex. *J. Biol. Chem.* **274**, 1646–1656 (1999).
42. Wang, A.V., Scholl, P.R. & Geha, R.S. Physical and functional association of the high affinity immunoglobulin G receptor (FcγRI) with the kinases Hck and Lyn. *J. Exp. Med.* **180**, 1165–1170 (1994).
43. Boyle, K.B. *et al.* Class IA phosphoinositide 3-kinase β and δ regulate neutrophil oxidase activation in response to *Aspergillus fumigatus* hyphae. *J. Immunol.* **186**, 2978–2989 (2011).
44. Kawabuchi, M. *et al.* Transmembrane phosphoprotein Cbp regulates the activities of Src-family tyrosine kinases. *Nature* **404**, 999–1003 (2000).
45. Saito, K. *et al.* BTK regulates PtdIns-4,5–P2 synthesis: importance for calcium signaling and PI3K activity. *Immunity* **19**, 669–678 (2003).
46. Condliffe, A.M. *et al.* Sequential activation of class IB and class IA PI3K is important for the primed respiratory burst of human but not murine neutrophils. *Blood* **106**, 1432–1440 (2005).
47. Uckun, F.M. *et al.* Anti-breast cancer activity of LFM-A13, a potent inhibitor of Polo-like kinase (PLK). *Bioorg. Med. Chem.* **15**, 800–814 (2007).
48. Mahajan, S. *et al.* Rational design and synthesis of a novel anti-leukemic agent targeting Bruton's tyrosine kinase (BTK), LFM-A13 [alpha-cyano-β-hydroxy-β-methyl-N-(2,5-dibromophenyl)propenamide]. *J. Biol. Chem.* **274**, 9587–9599 (1999).

ONLINE METHODS

Reagents and antibodies. The following reagents were used: lipopolysaccharide derived from *Escherichia coli* or *Pseudomonas aeruginosa*, fMLP, PMA, DHR123, luminol, N-acetyl cysteine, aprotinin, leupeptin, pepstatin and phenylmethyl sulfonyl fluoride (all from Sigma-Aldrich); recombinant human TNF (R&D Systems); Pam_3CSK_4, LFM-A13, LFM-A11, Syk inhibitor, FAK inhibitor and Ly294002 (all from Calbiochem); and dasatinib, IC87114 and AS-605240 (all from Biovision). Oligodeoxynucleotide CpG-A (5′-GGT GCATCGATGCAGGGGGG-3′) was from Operon Biotechnologies.

The antibodies used were as follows: goat polyclonal antibody to PI(3)K-p85α phosphorylated at Tyr508 (sc-12929), Hck phosphorylated at Tyr411 (sc-12928), rabbit polyclonal antibody to Hck (N-30), anti-PTEN (FL-403), anti-PTP-PEST (H130), anti-FAK (A-17), anti-Vav (C-14), anti-Syk (C-20), anti-SHP2 (C-18) and anti-SHP 1 (C-19), as well as mouse monoclonal antibody (mAb) to $p47^{phox}$ (D-10), $p40^{phox}$ (D-8) or $p22^{phox}$ (CS-9; all from Santa Cruz). Rabbit polyclonal antibody to p101-PI(3)K (07-281) and to $gp91^{phox}$ (07-024) and anti-Rac2 (07-604), biotin-labeled mouse mAb to phosphorylated tyrosine (4G10), as well as horseradish peroxidase–conjugated antibody to goat IgG (AP-180P) were from Upstate; fluorescein isothiocyanate–conjugated mouse mAb to gp91 (7D5) or goat antibody to mouse IgG (238) were from MBL; and mouse mAb to flotillin-1(18), $p67^{phox}$ (29) or PI(3)K-p85 (U15), and fluorescein isothiocyanate–conjugate mouse isotype-matched IgG antibody (MOPC-21) was from BD Pharmingen. Rabbit polyclonal antibody to PI(3)K-p85 (4292), to Lyn (2732), to Lyn phosphorylated at Tyr507 (2731), to Syk phosphorylated Tyr525-Tyr526 (2711), to Src phosphorylated Tyr416 (2101), to FAK phosphorylated Tyr576-Tyr577 (3281), to $p40^{phox}$ phosphorylated at Thr154 (4311) and to caspase-3 (9662), as well as mouse mAb to proliferating cell nuclear antigen (PC-19), were from Cell Signaling. Rabbit mAb to SOD1 (ep1727y), Mal (ep1231y) and catalase (ep1929), as well as rabbit polyclonal antibody to SOD2 (NB100-1992) and to Yes (NBP1-85369), were from Novus Biologicals. Rabbit polyclonal antibody to Bmx (ab73887), to Bmx phosphorylated at Tyr566 (ab59409), to Lyn phosphorylated at Tyr396 (EP503Y), to Vav phosphorylated at Tyr160 (ab4763) and to Prx1 (ab15571), and mouse mAb to Prx2 (12B1), as well as rabbit mAb to Btk (Y440), to CSK (CSK-04), to SHIP (EP378Y) and to Tec (Y398), were from Abcam. Rat mAb to Mal (TIRAP; sebi-1) was from ENZO Life Sciences. Goat polyclonal antibody to CBP (LS-C14699) was from LIFESPAN; anti-β-actin (Ab1) was from Calbiochem; and horseradish peroxidase–conjugated antibody to mouse IgG (NA931), to rabbit IgG (NA934) or to rat IgG (NA9350) was from GE Healthcare. Alexa Flour 546–anti–rabbit IgG (A11035), Alexa Flour 680–anti–rabbit IgG (A10043), Alexa Flour 594–anti–rat IgG (A21209) and Alexa Flour 488–anti–mouse IgG (A21202) were from Invitrogen. Mouse IgG (015-000-003) and rabbit IgG (011-00000-3) were from Jackson ImmunoResearch. Rat IgG2a (eBR2a) was from eBioscience. Horseradish peroxidase–conjugated streptavidin was from Cell Signaling.

The 482H mAb to Btk has been described[49]. Polyclonal antibody to human Btk was raised in rabbits with a Btk peptide of amino acids 169–187 (ENRNGSLKPGSSHRKTKKPC) conjugated to ovalubumin. The antibody collected was further affinity-purified with that same Btk peptide conjugated to thiol–Sepharose 4B (Pharmacia) and was used for immunoprecipitation in some experiments. The specificity of the antibody was confirmed by immunoblot analysis of lysates of Btk-deficient mononuclear cells. Antibody to phosphorylated Ser345 was generated in rabbits by injection of ovalbumin conjugated to a peptide of $p47^{phox}$ phosphorylated at Ser345 (QARPGPQSpPGSPLEEE, where 'Sp' indicates phosphorylated Ser345 (p-Ser345-pep)). The antibody raised was positively affinity-purified with activated thiol–Sepharose 4B adsorbed with p-Ser345-pep. The antibody was further purified by elimination of the fraction that bound to the same peptide of $p47^{phox}$ without phosphorylation at Ser345 (QARPGPQSPGSPLEEE (Ser345-pep)) by passage through thiol–Sepharose 4B conjugated to Ser345-pep; then, the antibody was used for immunoblot analysis. The specificity of the antibody was confirmed by direct enzyme-linked immunosorbent assay with plates coated with Ser345-pep or p-Ser345-pep and by immunoblot analysis experiments showing blockade of the p-$p47^{phox}$ signal by p-Ser345pep but not by Ser345-pep.

Subjects. Patients with XLA (n = 17) with stable health were studied (ages and Btk mutations, **Supplementary Fig. 3**). Healthy volunteers (n = 18) and patients with CVID (n = 5) were enrolled as healthy controls and disease control, respectively. Written informed consent was obtained from all subjects (or their parents). The study protocol was approved by the ethics committee of the Faculty of Medicine, Tokyo Medical and Dental University.

Isolation of neutrophils, monocytes and lymphocytes. Neutrophils were purified from heparinized peripheral blood by a standard technique. All samples were processed within 12 h of blood collection. Peripheral blood diluted in PBS was layered onto a MonoPoly mixture (Flow Laboratories) and centrifuged at 400*g* for 20 min. Layers with enrichment for neutrophils were collected and further purified to a purity of >97% by immunomagnetic negative selection (StemCell Technologies). Sterile and endotoxin-free conditions were used for all procedures. Monocytes were purified from the mononuclear cell–rich fraction with a human monocyte enrichment kit (StemCell Technologies), and lymphocytes were prepared as described[50].

Measurement of production of ROS. Purified neutrophils were loaded for 5 min at 37 °C with DHR123 (5 μg/ml). Cells were washed and then stimulated for 30 min at 37 °C with PMA (100 ng/ml), and the production of ROS was quantified via flow cytometry by measurement of intracellular rhodamine (FACSCalibur; Becton Dickinson). DHR123-loaded neutrophils were also stimulated for 60 min at 37 °C with a TLR ligand (lipopolysaccharide from *E. coli* or *P. aeruginosa*; 100 ng/ml), CpG-A (100 ng/ml) or TNF (1 μg/ml). After incubation, treated and untreated neutrophils were incubated for 5 min at 37 °C with or without fMLP (1 μM), followed by flow cytometry. Results are presented as MFI of treated cells – MFI of untreated cells.

Production of ROS was quantified by standard chemiluminescence. Neutrophils (1.0×10^6) were suspended in 0.5 ml PBS containing luminol (10 μM) preheated to 37 °C. After a baseline measurement was obtained, cells were stimulated with a TLR agonist and then with fMLP (1 μM) or with PMA (100 ng/ml); luminescence signals were monitored throughout the reaction.

Detection of apoptosis. Apoptotic cells were identified by staining with annexin V–fluorescein isothiocyanate and 7-AAD (7-amino-actinomycin D; BD Biosciences). Apoptosis was also identified by immunoblot analysis through the detection of cleaved caspase-3 or degraded proliferating cell nuclear antigen.

Flow cytometry. A FACSCalibur (Beckton Dickenson) was used for all flow cytometry analyzing surface expression of gp91, DHR123 staining, annexin V–7-AAD staining, and JC-1 mitochondrial membrane detection as described[50]. All analyses were undertaken after calibration of the fluorescence intensity with CaliBRITE Beads (BD Biosciences).

Subcellular fractionation of neutrophils. Isolated neutrophils were resuspended at a density of 5×10^7 cells per ml in ice-cold sonication buffer (HEPES (10 mM), pH 7.2, sucrose (0.15 M), EGTA (1 mM), EDTA (1 mM), NaF (25 mM), leupeptin (10 μg/ml), pepstatin (10 μg/ml), aprotinin (1 μg/ml) and PMSF (1 mM)). After sonication and pelleting on ice, 200 μl supernatant was layered on a discontinuous sucrose gradient consisting of 200 μl of 52% (wt/vol) sucrose, 200 μl of 40% (wt/vol) sucrose and 200 μl of 15% (wt/vol) sucrose. After centrifugation (100,000*g* for 60 min), 160 μl supernatant (cytosol source) and 120 μl interface of the 15%–40% sucrose layers (plasma-membrane source) were collected.

Immunoprecipitation and immunoblot analysis. Lysates were prepared from monocytes and lymphocytes as described[51]. For the preparation of lysates from neutrophils, cells were resuspended in lysis buffer (Tris-HCl (50 mM), pH 7.5, NaCl (150 mM), sucrose (0.25 M), EGTA (5 mM), EDTA (5 mM), leupeptin (15 μg/ml), pepstatin (10 μg/ml), aprotinin (10 μg/ml), PMSF (2.5 mM), 1.0% Nonidet-P40, 0.25% sodium deoxycholate, sodium pyrophosphate (10 mM), NaF (25 mM), Na_3VO_4 (5 mM), β-glycerophosphate (25 mM) and DNase I (1 μg/ml)), incubated for 30 min on ice and centrifuged at 15,000*g* for 30 min at 4 °C, then supernatants were collected. For extraction of the membrane-raft fraction, 1% n-dodecyl-β-D-maltoside was added to the lysis buffer. Immunoprecipitation and immunoblot analysis were done as described[52]. For immunoprecipitation of cytosolic proteins from neutrophils, cytosolic proteins

doi:10.1038/ni.2234

obtained as described above were diluted in four volumes of immunoprecipitation buffer (Tris-HCl (20 mM), pH 7.5, NaCl (150 mM), sucrose (0.25 M), EGTA (5 mM), EDTA (5 mM), leupeptin (15 μg/ml), pepstatin (10 μg/ml), aprotinin (10 μg/ml), PMSF (2.5 mM), 0.5% Triton-X, sodium pyrophosphate (10 mM), NaF (25 mM), Na_3VO_4 (5 mM), β-glycerophosphate (50 mM) and levamisole (1 mM)); supernatants were used for immunoprecipitation.

Measurement of phosphatidylinositol-(3,4,5)-trisphosphate. Phosphatidylinositol-(3,4,5)-trisphosphate in unstimulated neutrophils prepared from healthy controls and patients with XLA was measured with an enzyme-linked immunosorbent assay kit in accordance with the manufacturer's instructions (K-2500; Echelon).

Immunofluorescence staining. Cytospin preparations of neutrophils were air-dried and fixed for 10 min with paraformaldehyde in PBS, pH 7.4, then were made permeable for 20 min at −20 °C with acetone, washed, and incubated with the appropriate antibodies. After labeling and washing with 0.2% BSA in PBS, coverslips were mounted with Fluoromount G and the prepared specimens. Nuclei were counterstained with DAPI (4,6-diamidino-2-phenylindole). Slides were analyzed with a fluorescence microscope (FV10i; Olympus) equipped with Fluoview viewer and review station (Olympus). At least 100 cells were inspected for each slide.

Generation of Hph-1-Btk, Hph-1-Btk mutants, and transduction of recombinant protein into cells. Hph-1–tagged Btk constructs were generated by amplification of a full-length Btk cDNA fragment with the appropriate primers (**Supplementary Table 1a**). After the sequence of each PCR product was verified by DNA sequencing, the fragment was ligated into sites of a pET28b vector (Merck) cleaved by *Xmal* and *Sall*; the vector has a six-histidine site for protein purification and two tandem Hph-1 sequences for protein transduction. Constructs with deletion of the Tec homology domain, SH3 domain or SH2 domain were generated by mutagenesis with the QuikChange SiteDirected Mutagenesis Kit (Stratagene) and the appropriate primers (**Supplementary Table 1b**). The Hph-1-Gal4 construct has been described[52]. Proteins were induced in BL21 Star competent cells (Novagen) as described[52]. Proteins were treated with Detoxi-Gel Endotoxin Removing Gel (Takara Bio) for elimination of endotoxins and were frozen at −80 °C until further use. Neutrophils (1×10^6 per ml) were incubated for 1 h with 1 μM Hph-1–tagged proteins (80 μg recombinant Hph-1–tagged full-length-Btk was used for 1×10^6 neutrophils for transduction at a concentration of 1 μM) and washed, then ROS production was assayed.

Btk-precipitation assay. Lysates of neutrophils from healthy controls were prepared on ice for 30 min with immunoprecipitation lysis buffer. Supernatants were then treated with protein G beads (GE Health Care) for removal of immunoglobulin G from the neutrophil lysate. For the Btk-precipitation assay, purified Btk recombinant proteins or control recombinant protein were eluted and proteins were measured by BCA protein assay (Pierce). Bacterial supernatants were bound to nickel–nitrilotriacetic acid Sepharose beads (Qiagen) and bound recombinant proteins were eluted, then equimolar amounts of recombinant proteins were rebound to the nickel beads; afterward, samples were washed and then incubated overnight at 4 °C with the cell lysates. Beads were washed four times with lysis buffer and assessed by immunoblot analysis with anti-Mal. Before incubation with cell lysates, the amount of the recombinant protein rebound to nickel beads was assessed by immunoblot analysis with anti-histidine, and the 'dose' was readjusted for further precipitation assays.

Statistical analysis. Student's *t*-test was used for statistical analysis. The software GraphPad Prism 4 was used for these analyses.

49. Futatani, T. *et al.* Deficient expression of Bruton's tyrosine kinase in monocytes from X-linked agammaglobulinemia as evaluated by a flow cytometric analysis and Its clinical application to carrier detection. *Blood* **91**, 595–602 (1998).
50. Takahashi, N. *et al.* Impaired CD4 and CD8 effector function and decreased memory T cell populations in ICOS-deficient patients. *J. Immunol.* **182**, 5515–5527 (2009).
51. Morio, T. *et al.* Ku in the cytoplasm associates with CD40 in human B cells and translocates into the nucleus following incubation with IL-4 and anti-CD40 mAb. *Immunity* **11**, 339–348 (1999).
52. Choi, J.M. *et al.* Intranasal delivery of the cytoplasmic domain of CTLA-4 using a novel protein transduction domain prevents allergic inflammation. *Nat. Med.* **12**, 574–579 (2006).

doi:10.1038/ni.2234

GATA-2 *anomaly and clinical phenotype of a sporadic case of lymphedema, dendritic cell, monocyte, B- and NK-cell (DCML) deficiency, and myelodysplasia*

Hiroyuki Ishida, Kosuke Imai, Kenichi Honma, Shin-ichi Tamura, Toshihiko Imamura, Masafumi Ito & Shigeaki Nonoyama

European Journal of Pediatrics

ISSN 0340-6199

Eur J Pediatr
DOI 10.1007/s00431-012-1715-7

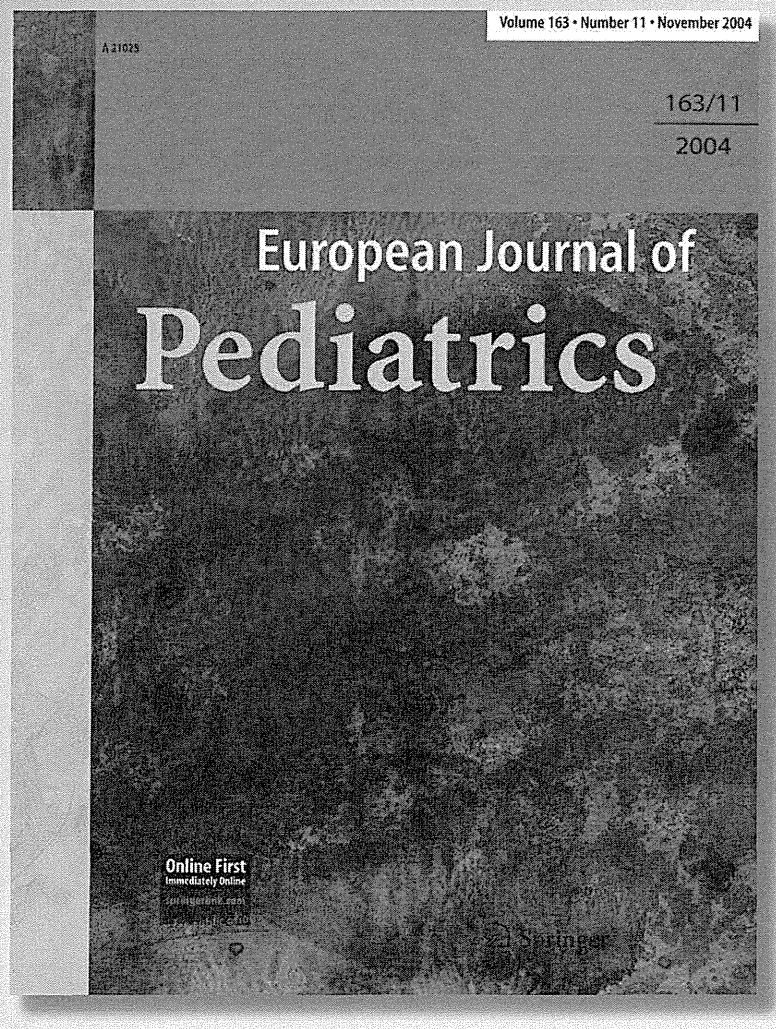

Springer

Eur J Pediatr
DOI 10.1007/s00431-012-1715-7

CASE REPORT

GATA-2 anomaly and clinical phenotype of a sporadic case of lymphedema, dendritic cell, monocyte, B- and NK-cell (DCML) deficiency, and myelodysplasia

Hiroyuki Ishida · Kosuke Imai · Kenichi Honma · Shin-ichi Tamura · Toshihiko Imamura · Masafumi Ito · Shigeaki Nonoyama

Received: 14 December 2011 / Accepted: 29 February 2012

Abstract A Japanese patient presented with lymphedema, severe *Varicella zoster*, and *Salmonella* infection, recurrent respiratory infections, panniculitis, monocytopenia, B- and NK-cell lymphopenia, and myelodysplasia. The phenotype was a mixture of the monocytopenia and mycobacterial infection (MonoMAC) and Emberger syndromes. Sequencing of the *GATA-2* cDNA revealed the heterozygous missense mutation 1187 G>A. This mutation resulted in the amino acid mutation Arg396Gln in the zinc fingers-2 domain, which is predicted to cause significant structural change and prevent a critical interaction with DNA. Functional analysis of the patient's *GATA-2* mutation is required to understand the relationship between these distinctive syndromes.

Keywords Emberger syndrome · MonoMAC · Monocytopenia · B- and NK-cell lymphopenia · Immunodeficiency · Myelodysplasia

H. Ishida (✉) · S.-i. Tamura
Department of Pediatrics and Blood and Marrow transplantation,
Matsushita Memorial Hospital,
5-55, Sotojima-cho,
Moriguchi 570-8540, Japan
e-mail: ishida.hiroyuki002@jp.panasonic.com

H. Ishida
e-mail: ishidah@koto.kpu-m.ac.jp

K. Imai
Department of Pediatrics, Tokyo Medical and Dental University,
5-45 Yushima 1-Chome,
Bunkyo-Ku, Tokyo 113-8510, Japan

K. Honma · S. Nonoyama
Department of Pediatrics, National Defense Medical College,
3-2 Namiki,
Tokorozawa 359-8513, Japan

T. Imamura
Department of Pediatrics,
Kyoto Prefectural University of Medicine,
465 Kajii-Cho, Kawaramachi-Hirokoji,
Kamigyo-Ku, Kyoto 602-8566, Japan

M. Ito
Department of Pathology,
Japanese Red Cross Nagoya First Hospital,
3-35 Michishita-cho, Nakamura-ku,
Nagoya 453-0046, Japan

Recent studies have characterized a novel primary immunodeficiency known as monocytopenia and mycobacterial infection (MonoMAC), also known as dendritic cell, monocyte, B and NK lymphoid (DCML) deficiency. This form of immunodeficiency occurs either as an autosomal dominant form or sporadically. It is primarily characterized by persistent and profound peripheral monocytopenia, diagnostic B- and NK-cell lymphocytopenia, and variable T cell lymphocytopenia, along with increased susceptibility to mycobacterium or papilloma virus infections [1, 2, 13]. Moreover, most patients with MonoMAC eventually develop acute myelogenous leukemia (AML) following myelodysplastic syndrome (MDS). Another rare disorder called Emberger syndrome (MIM614038) is characterized by congenital deafness and primary lymphedema of the lateral lower limb; typically, onset occurs in childhood and is associated with a predisposition to MDS or AML in addition to other minor anomalies such as hypotelorism and long tapering fingers. It is also a sporadic or familial disorder [8]. Familial MDS/AML without other hematopoietic defects has also been reported [6]. Surprisingly, it was reported recently that these three distinctive syndromes are all caused by *GATA-2*

Published online: 21 March 2012

mutations, which suggests that these syndromes are different phenotypes caused by the same genetic alteration [5–7, 9]. Here, we report the case of a patient with a *GATA-2* mutation bearing the characteristic features of MonoMAC/Emberger syndrome.

Case report

The patient was the second child of non-consanguineous parents. Neither the parents nor the elder brother had a history of increased susceptibility to infection. The medical history of the patient included BCG vaccination 3 months after birth without any side effects and a severe *Varicella zoster* infection at 2 years of age. After that, she suffered repeated upper and lower respiratory tract infections that required antibiotics. At 4 years of age, the patient's peripheral blood showed mild neutropenia and profound monocytopenia ($0–20\times10^6$/L), and mild hypocellularity but no dysplasia was observed in the bone marrow. At 8 years of age, she experienced a prolonged *Salmonella* enterocolitis infection. Lymphedema in the left leg first appeared at 13 years of age. She subsequently developed recurrent panniculitis. Recently, the patient (now 19 years old) was admitted to hospital with fever (with no apparent cause) and panniculitis (Fig. 1a). She had mild hypotelorism and lymphedema, with warts on her left leg (Fig. 1b). Her mental ability was appropriate for her age. An immunodeficiency was first suspected after the severe *Varicella zoster* and *Salmonella* infections during early childhood. The most recent recurrent episode of fever supported this suspicion.

Peripheral blood analysis revealed a white blood cell count of 1.5×10^9/L with 45% neutrophils, 54 % lymphocytes, and 1 % monocytes, a hemoglobin level of 11.0 g/dl, and a platelet count of 146×10^9/L. Flow cytometric analysis of the peripheral blood also revealed a deficiency in dendritic cells (lineage$^-$/DR$^+$/CD123$^+$ or CD11c$^+$ cells, 0%), B cells (CD19$^+$ cells, 0.7%), and NK cells (CD3$^-$/CD56$^+$ cells, 0.5%), and profound monocytopenia (CD14$^+$ cells, 0.2%). Lymphocytes comprised 97% T cells (CD4/8 ratio, 0.54), 33% of which were TCR $\gamma\delta^+$ T cells. Immunological analyses revealed IgG, IgA, IgM, and IgE levels of 711, 65, 131,

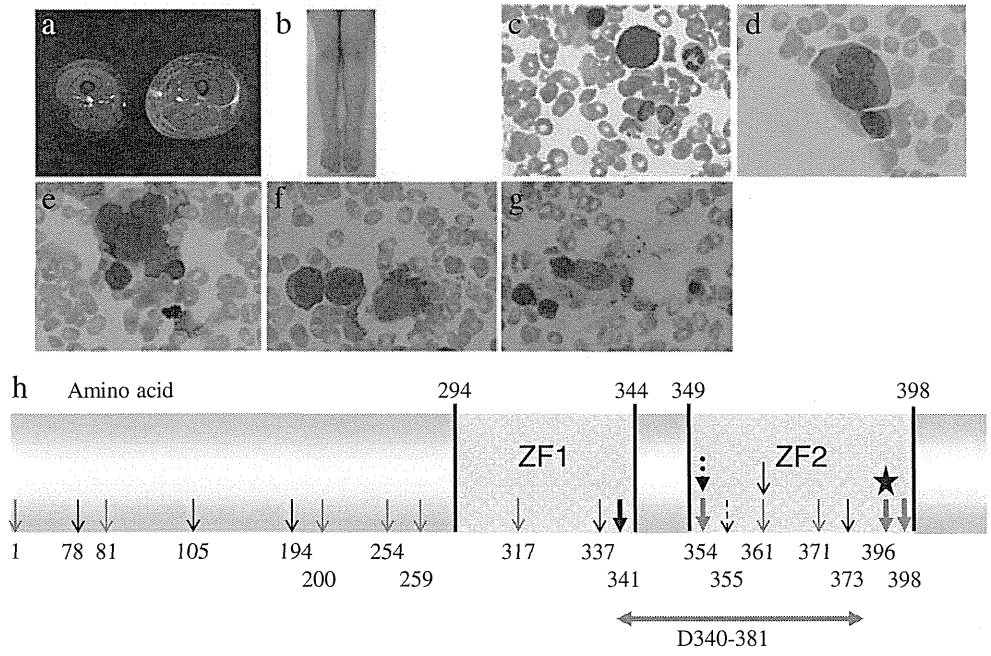

Fig. 1 Clinical and bone marrow features and *GATA-2* protein mutation sites. **a** A gadolinium-enhanced T2-weighted MRI image of the left thigh was performed when the patient developed panniculitis at 19 years of age. An increased signal was observed in the subcutaneous tissue and fascial layers. **b** After she was cured, the patient showed lymphedema in her left leg. **c–g** Bone marrow taken at the same time revealed decreased granule numbers within neutrophils and a pseudo-Pelger anomaly (**c**), binucleation (**d**), and megaloblastic changes in erythroblasts, dysplastic nuclei in megakaryocytes (**e**) and micromegakaryocytes (**f**), and hemophagocytosis (**g**). **h** Depiction of the *GATA-2* protein mutations previously identified in MonoMAC/DCML deficiency and Emberger syndrome. ZF1 and ZF2 are functional DNA-binding domains. The *star* indicates the Arg396Gln mutation identified in the present case. *Arrows* indicate previously reported mutations. These include missense, nonsense, and frameshift mutations (*short downward arrows*, respectively) and long deletions (*horizontal arrows*). *Black arrows* denote mutations associated with Emberger syndrome, *gray arrows* denote mutations associated with MonoMAC syndrome/DCML deficiency, *long horizontal arrows* indicate long deletions that have been observed in MonoMAC syndrome/DCML deficiency, *broken black arrows* denote mutations associated with familial MDS/AML, and *bold arrows* denote multiple pedigrees with the same mutation

and 5 mg/dl, respectively, and lymphocyte stimulation responses to phytohemagglutinin at the lower limits of the normal range. Antibody memory responses to infections contracted in early childhood (*Varicella* and *measles*) were maintained, and fibroblast sensitivity to radiation was normal. Flow FISH analysis of peripheral blood lymphocytes revealed normal telomere length; however, the peripheral blood contained 160 copies/μg WT1-mRNA (the upper limit of normal is 50 copies/μg RNA), and bone marrow aspirates showed hypocellularity, particularly of myeloid and lymphoid cells. Strikingly, despite monocytopenia in the peripheral blood, $CD64^+$ macrophages (accompanied by a few hemophagocytes) were observed in bone marrow specimens. Significant trilineage dysplasia was also present (Fig. 1c–g). Cytogenetic and chromosomal breakage analyses showed normal results. Meanwhile, profiles of familial peripheral blood showed a white blood cell count of 5.6×10^9/L with 50% neutrophils, 30% lymphocytes, and 8% monocytes, a hemoglobin level of 15.1 g/dl, and a platelet count of 199×10^9/L in the father; 5.1×10^9/L with 51 % neutrophils, 36% lymphocytes, and 9% monocytes, 10.7 g/dl, and 225×10^9/L in the mother; and 6.6×10^9/L with 41% neutrophils, 45% lymphocytes, and 10% monocytes, 15.4 g/dl, and 208×10^9/L in the brother. Flow cytometric analysis of peripheral blood samples taken from these family members showed a normal frequency of B cells ($CD19^+$ cells) and NK cells ($CD3^-/CD56^+$ cells) (the father 11 and 8%, the mother 10 and 12%, and the brother 9 and 15%, respectively). Taken together, these findings suggested that the patient might have sporadic MonoMAC/Emberger syndrome.

Sequencing of *GATA-2* cDNA revealed a 1187 G>A heterozygous missense mutation. This mutation resulted in an Arg396Gln substitution in the zinc finger-2 domain, which is predicted to cause significant structural changes that prevent critical interactions with DNA (Fig. 1h). Furthermore, sequencing of cDNA from her healthy familial members revealed no mutations, including 1187 G>A in *GATA-2* gene. Ultimately, the patient was diagnosed with MonoMAC/Emberger syndrome with a de novo *GATA-2* mutation.

Discussion

GATA-2 plays a critical role in both hematopoietic stem cell development and the maintenance of normal adult stem cell homeostasis [10]. It is likely that the significant protein structural alterations caused by mutations in *GATA-2* result in loss-of-function or have a dominant-negative effect on the DNA-binding ability of wild-type *GATA-2* [9] It seems reasonable to suggest that the loss of hematopoiesis-indispensable transcription factor activity results in impaired hematopoietic-cell differentiation and hematopoietic stem cell exhaustion; this in turn may promote the development of related diseases such as MDS and AML. Additional genetic alterations may also be required.

The patient's phenotype included hypotelorism, primary lymphedema (which had an onset during childhood before the recurrent episodes of panniculitis), peripheral monocytopenia, B- and NK-cell lymphocytopenia, neutropenia since early childhood, and myelodysplasia. The Arg396Glu mutation in *GATA-2* identified in this patient was not detected in 150 healthy individuals [7]. Taken together, these factors confirmed the diagnosis of MonoMAC/Emberger syndrome with a de novo *GATA-2* mutation; however, the *GATA-2* mutations alone cannot explain the phenotypic diversity between these three syndromes (MonoMAC, Emberger syndrome, and familial MDS/AML) and the presented patient. Interestingly, she developed neither BCG dissemination nor severe lymphadenitis after her BCG

Table 1 Summary of the clinical features of MonoMAC, Emberger syndrome, and the present case

	MonoMAC/DCML deficiency	Emberger syndrome	Present case
DCML[a] deficiency	+	+/–	+
MDS/AML	+	+	+
Lymphedema	ND	+	+
Deafness	ND	+/–	–
Hypotelorism	ND	+/–	+
Long slender fingers	ND	+/–	–
Mycobacterial infection	+	ND	–
Fungal infection	+/–	+/–	–
Papillomaviral infection/warts	+	+	+
Severe *varicella* and/or *Salmonella* infection	+/–	ND	+
Pulmonary alveolar proteinosis	+/–	ND	–
Panniculitis/erythema nodusa	+/–	+/–	+

ND not described, *MDS* myelodysplastic, *AML* acute myelogenous syndrome, + most cases, +/– some cases

[a]Dendritic cell, monocyte, B and NK lymphoid syndrome

vaccination 3 months after birth. This indicates normal functioning of tissue macrophages, because protective immunity to mycobacteria is dependent upon the interleukin (IL)-12/IL-23-interferon (IFN)-γ axis, possibly mediated by intracellular killing of phagocytes following the production of IFN-γ by CD4 T lymphocytes in response to IL-12/IL-23 secreted by infected macrophages [3]. Patients with MonoMAC/DCML deficiency show very low numbers of circulating monocytes and no detectable myeloid or plasmacytoid dendritic cells in the peripheral blood, but relatively normal numbers of Langerhans cells and tissue macrophages accompanied by prominent hemophagocytosis in the bone marrow [1, 2]. This supports the idea that tissue and marrow macrophages, in addition to Langerhans cells, may be maintained by a distinct precursor from circulating monocytes or dendritic cells [1].

Mansour et al. [8] reported that the age of onset of MDS/AML in Emberger syndrome is 9–14 (median 11) years of age. This appears to be earlier than that of MDS/AML in MonoMAC syndrome (7–52 years, median 32 years) [2]. Moreover, the level of WT1-mRNA in the peripheral blood increases significantly as MDS progresses and is a strong predictor of rapid AML transformation in adult patients with de novo MDS [11]. The level of WT1-mRNA in the peripheral blood of the current patient was as high as that in patients that show worse survival than those with a low level WT1 mRNA (10^2–10^4 vs. $<10^2$ copies/μg) [12]. However, it is unclear whether phenotypic variation and increased WT1 mRNA level are related to hematological disease progression. In any case, neutropenic patients who suffer recurrent infections and/or MDS are likely to need a transplant in the near future. Therefore, for such cases, we perform hematopoietic stem cell transplantation with a reduced intensity conditioning regimen before the disease has progressed [4]. Table 1 summarizes the clinical features of MonoMAC, Emberger syndrome, and the present case.

Our observations suggest that children with recurrent or prolonged common infections that respond to antibiotics and recover well may suffer from unknown primary immunodeficiencies. Although the relationship between *GATA-2* and lymphedema or deafness requires further investigation, tissue-specific lesions such as lymphedema provide important clues to primary immunodeficiencies that also affect non-hematopoietic cells.

Acknowledgments We are grateful to Dr. Sayoko Doisaki in the Department of Pediatrics, Nagoya University of Medical School, for the flow FISH analysis.

Conflict of Interest Statement The authors declare no competing financial interests.

References

1. Bigley V, Haniffa M, Doulatov S, Wang XN, Dickinson R, McGovernet N et al (2011) The human syndrome of dendritic cell, monocyte, B and NK lymphoid deficiency. J Exp Med 208:227–234
2. Calvo KR, Vinh DC, Maric I, Wang W, Noel P, Stetler-Stevenson M, Holland SM et al (2011) Myelodysplasia in autosomal dominant and sporadic monocytopenia immunodeficiency syndrome: diagnostic features and clinical implications. Haematologica 96:1221–1225
3. Carneiro-Sampaio M, Coutinho A (2007) Immunity to microbes: lessons from primary immunodeficiencies. Infect Immun 75:1545–1555
4. Cuellar-Rodriguez J, Gea-Banacloche J, Freeman AF, Hsu AP, Zerbe CS, Calvo KR et al (2011) Successful allogeneic hematopoietic stem cell transplantation for GATA2 deficiency. Blood 118:3715–3720
5. Dickinson RE, Griffin H, Bigley V, Reynard LN, Hussain R, Haniffa M et al (2011) Exome sequencing identifies *GATA-2* mutation as the cause of dendritic cell, monocyte, B and NK lymphoid deficiency. Blood 118:2656–2658
6. Hahn CN, Chong CE, Carmichael CL, Wilkins EJ, Brautigan PJ, Li XC et al (2011) Heritable GATA2 mutations associated with familial myelodysplastic syndrome and acute myeloid leukemia. Nat Genet 43:1012–1017
7. Hsu AP, Sampaio EP, Khan J, Calvo KR, Lemieux JE, Patel SY et al (2011) Mutations in GATA2 are associated with the autosomal dominant and sporadic monocytopenia and mycobacterial infection (MonoMAC) syndrome. Blood 118:2653–2655
8. Mansour S, Connell F, Steward C, Ostergaard P, Brice G, Smithson S et al (2010) Lymphoedema research consortium. Emberger syndrome-primary lymphedema with myelodysplasia: report of seven new cases. Am J Med Genet A 152A:2287–2296
9. Ostergaard P, Simpson MA, Connell FC, Steward CG, Brice G, Woollard WJ et al (2011) Mutations in GATA2 cause primary lymphedema associated with a predisposition to acute myeloid leukemia (Emberger syndrome). Nat Genet 43:929–931
10. Rodrigues NP, Boyd AS, Fugazza C, May GE, Guo Y, Tipping AJ et al (2008) *GATA-2* regulates granulocyte-macrophage progenitor cell function. Blood 112:4862–4873
11. Tamaki H, Ogawa H, Ohyashiki K, Ohyashiki JH, Iwama H, Inoue K et al (1999) The Wilms' tumor gene WT1 is a good marker for diagnosis of disease progression of myelodysplastic syndromes. Leukemia 13:393–399
12. Tamura H, Dan K, Yokose N, Iwakiri R, Ohta M, Sakamaki H et al (2010) Prognostic significance of WT1 mRNA and anti-WT1 antibody levels in peripheral blood in patients with myelodysplastic syndromes. Leuk Res 34:986–990
13. Vinh DC, Patel SY, Gl U, Anderson VL, Freeman AF, Olivier KN et al (2010) Autosomal dominant and sporadic monocytopenia with susceptibility to mycobacteria, fungi, papillomaviruses, and myelodysplasia. Blood 115:1519–1529

Clinical Endocrinology (2012) 77, 628–634 doi: 10.1111/j.1365-2265.2012.04390.x

ORIGINAL ARTICLE

Endocrine complications in primary immunodeficiency diseases in Japan

Takafumi Nozaki*, Hidetoshi Takada*, Masataka Ishimura*, Kenji Ihara*, Kohsuke Imai†, Tomohiro Morio†, Masao Kobayashi‡, Shigeaki Nonoyama§ and Toshiro Hara*

*Department of Pediatrics, Graduate School of Medical Sciences, Kyushu University, Fukuoka, †Department of Pediatrics and Developmental Biology, Graduate School of Medical and Dental Sciences, Tokyo Medical and Dental University, Tokyo, ‡Department of Pediatrics, Graduate School of Biomedical Sciences, Hiroshima University, Hiroshima, and §Department of Pediatrics, National Defense Medical College, Tokorozawa, Japan

Summary

Background In spite of the accumulating evidence on the interaction between the immune and endocrine systems based on the recent progress in molecular genetics, there have been few epidemiological studies focused on the endocrine complications associated with primary immunodeficiency diseases (PID).

Objective To investigate the prevalence and clinical features of endocrine complications in patients with PID in a large-scale study.

Design and participants This survey was conducted on patients with PID who were alive on 1 December 2008 and those who were newly diagnosed and died between 1 December 2007 and 30 November 2008 in Japan. We investigated the prevalence and the clinical data of the endocrine complications in 923 patients with PID registered in the secondary survey.

Results Among 923 PID patients, 49 (5·3%) had endocrine disorders. The prevalence of the endocrine diseases was much higher in patients with PID than in the general population in the young age group, even after excluding patients with immune dysregulation.

Conclusions Endocrine disorders are important complications of PID. Analysis of the endocrine manifestations in patients with PID in a large-scale study may provide further insights into the relationship between the immune and endocrine systems.

(Received 15 November 2011; returned for revision 23 December 2011; finally revised 19 January 2012; accepted 13 March 2012)

Introduction

A wide variety of clinical complications have been described in primary immunodeficiency diseases (PID).[1,2] PID have been reported to be associated with an increased risk of cancer, in particular non-Hodgkin lymphoma,[2] and the contribution of immune dysfunction in PID to cancer risk is receiving much attention. It is also well known that patients with PID often have complications such as autoimmune and allergic disorders.[1,3] Recently, the interaction between the immune and endocrine systems has been getting increasing attention.[4,5] However, there have so far been no reports focusing on the endocrine complications associated with PID in a large-scale survey.

Many endocrine disorders in patients with PID are thought to be due to the development of the autoimmunity, which is closely related to the pathophysiology of PID.[6] However, it is not known how the immunological and molecular defects in individual PID contribute to the development of various autoimmune endocrine disorders. In addition, the genetic defects in some PID can lead to these complications directly or indirectly via nonimmunological mechanisms.[6]

We analysed the endocrine complications in PID from the information obtained from the nationwide PID survey in Japan conducted in 2008. This is the first large-scale survey focusing on the endocrine complications in PID.

Materials and methods

This survey was performed according to the nationwide epidemiological survey manual of patients with intractable diseases (2nd edition 2006, Ministry of Health, Labour and Welfare of Japan) as described previously.[7] PID classification was based on the criteria of the International Union of Immunological Societies Primary Immunodeficiency Diseases Classification Committee in 2007.[8] The survey was conducted on patients with PID who were alive on 1 December 2008 and those who were newly diagnosed and died between 1 December 2007 and 30 November 2008 in Japan. The initial survey covered 1224 paediatric departments and 1670 internal medicine departments, which were randomly selected according to the number of beds among the 2291 paediatric departments and 8026 internal medicine departments in Japan. Primary questionnaires regarding the number of patients and the disease names based on the PID classification

Correspondence: Takafumi Nozaki, Department of Pediatrics, Graduate School of Medical Sciences, Kyushu University, 3-1-1 Maidashi, Higashi-ku, Fukuoka 812-8582, Japan. Tel.: +81 92 642 5421; Fax: +81 92 642 5435; E-mail: t-nozaki@pediatr.med.kyushu-u.ac.jp

were sent to the selected hospitals. The initial survey was conducted to investigate the prevalence of the respective PID. The secondary survey was performed to study the detailed clinical features of individual patients with PID. Secondary questionnaires regarding age, gender, clinical manifestations and complications other than those related to haematopoietic stem cell transplantation of individual patients with PID were sent to the respondents who answered that they observed at least one PID patient with characteristics listed in the primary questionnaires. The details of the methods of the questionnaire investigation, the response rates and the breakdown of the number of patients in both paediatric and internal medicine departments were described elsewhere.[9] The questionnaires were designed to elucidate the clinical characteristics including the manifestations and laboratory data of the patients. In this study, all endocrine manifestations in patients with PID were included as complications of PID, even if they were well known major symptoms of PID.

Results

Detailed clinical information was available from 923 (secondary survey) out of 1240 patients with PID (initial survey).[9] Among the 923 patients with PID, 49 (5·3%) had endocrine disorders. As shown in Table 1, more than two thirds of the patients with PID were <20 years old and the prevalence of endocrine diseases was much higher in the young population of patients with PID than that in the general young population,[7,10–14] even after excluding patients with immune dysregulation (PID category IV). As expected, hypoparathyroidism was the most common endocrine disorder, because it is very frequently observed in patients with DiGeorge syndrome. Endocrine manifestations were also common in patients with diseases of immune dysregulation, such as immune dysregulation, polyendocrinopathy, enteropathy, X-linked (IPEX) syndrome and autoimmune polyendocrinopathy-candidiasis-ectodermal dystrophy (APECED). Although the number of patients with defects in innate immunity was small, endocrine complications seemed to be more common than expected. Interestingly, endocrine disorders were not observed in patients with complement deficiencies. In addition, Graves' disease and Addison's disease were not observed in any of the patients with PID in this study.

Type 1 diabetes mellitus (T1D) was observed in six patients with PID (Tables 1 and 2) including four with type 1A (autoimmune) and two with type 1B (autoantibody-negative, idiopathic). Type 1A diabetes mellitus occurred frequently in patients with IPEX or IPEX-like syndrome (two of six patients, 33·3%) (Table 1). One patient of unknown aetiology in PID category IV showed type 1A diabetes and Hashimoto's thyroiditis along with recurrent viral infections (Tables 1, 2 and S1). In the cases of type 1A diabetes mellitus, anti-glutamic acid decarboxylase (GAD) autoantibodies and anti-insulin autoantibodies (IAA) were positive in all patients and in two of four patients, respectively (Table 2). The patients with IPEX and IPEX-like syndrome had a history of diabetic ketoacidosis with poor glycaemic control, and they developed T1D at a younger age than the other patients with PID. The first case of warts, hypogammaglobulinaemia, infections, and myelokathexis (WHIM) syndrome with T1D and hypothyroidism was included (Tables 2 and S2).[15] With regard to type 1B diabetes mellitus, the patient with hypogammaglobulinaemia of unknown aetiology had diabetic ketoacidosis (Table 2). On the other hand, type 2 diabetes mellitus (T2D) was observed in two patients with PID (Table 1).

Hashimoto's thyroiditis was observed in five patients with PID (Tables 1 and S1). The onset was very early in the patient with IPEX syndrome (at birth). All patients had at least 1 autoantibody among the anti-thyroid peroxidase (TPO), anti-thyroglobulin (Tg) and thyroid stimulating hormone receptor autoantibodies (TRAb).

Nonautoimmune hypothyroidism was reported in seven patients with PID (Tables 1 and S2). Anti-thyroid autoantibodies were all negative when measured. Among these, three patients with X-linked agammaglobulinaemia (XLA), IgG subclass deficiency or WHIM syndrome had primary (congenital) hypothyroidism detected by newborn mass screening. Hypothyroidism in the other four patients with normal TSH levels was considered to be due to central hypothyroidism, a disorder of the pituitary, hypothalamus or hypothalamic-pituitary portal circulation. Two patients with severe combined immunodeficiency (SCID) developed hypothyroidism before they received haematopoietic stem cell transplantation.

Growth hormone deficiency (GHD) was observed in six patients with PID (Tables 1 and S3), whose heights at the diagnosis of GHD ranged from −11·3 SD to −2·5 SD. Five patients were treated with growth hormone. One patient with SCID received cord blood transplantation when she was 20 months old, without conditioning chemotherapy or radiation.

Hypogonadism was observed in three patients with PID (Tables 1 and S4). Among them, two had hypergonadotrophic (primary) hypogonadism, whereas the other had hypogonadotrophic (central) hypogonadism. None of the patients received haematopoietic stem cell transplantation.

One common variable immunodeficiency disease (CVID) patient had isolated ACTH deficiency (Table 1). The other endocrine complications included hypophosphataemia, pseudohypoaldosteronism, adrenal crisis, hypoglycaemia and hypophosphataemic rickets as shown in Table 1.

Discussion

This is the first nationwide survey focusing on the endocrine complications of PID. Among these, hypoparathyroidism was the most common, observed in patients with DiGeorge syndrome and APECED.[16,17] In APECED, the calcium-sensing receptor has been reported to be the autoantigen responsible for hypoparathyroidism.[18] Although it has been reported that 79% of patients with APECED have hypocalcaemia due to hypoparathyroidism,[17] only 1 (25%) among four patients with APECED developed hypoparathyroidism in this study, which might be one of the clinical characteristics of patients with APECED in Japan.

The prevalence (33·3%) of T1D in patients with IPEX syndrome in this study seemed to be lower than that (>70%) of the previous reports.[19,20] The low prevalence of T1D might be due to

Table 1. Endocrine complications in PID patients

PID category	Hypopara-thyroidism	Diabetes mellitus			Thyroid disease		GHD	Hypogonadism	Isolated ACTH deficiency	Others	The number of PID patients			
		T1D			Autoimmune hypothyroidism (Hashimoto's thyroiditis)	Non-autoimmune hypothyroidism					*n*	0–19 years	Total	Percent in total
		1A	1B	T2D										
I. Combined T and B cell immunodeficiencies											**4**	**67**	**75**	**5·3**
RAG1 deficiency						1					1	6	6	16·7
CD4 deficiency					1						1	2	2	50·0
Undetermined											2	10	10	20·0
T-B-SCID						1	1				2	4	4	50·0
II. Predominantly antibody deficiencies											**13**	**231**	**378**	**3·4**
X-linked agammaglobulinaemia						1				2*	3	93	138	2·2
Common variable immunodeficiency disorders			1		1††		1		1	2†	6	29	93	6·5
IgG subclass deficiency						2					2	45	50	4·0
Undetermined			1				1**	1**			2	9	9	22·2
III. Other well-defined immunodeficiency syndromes											**20**	**126**	**165**	**12·1**
Hyper-IgE syndrome							1	1		1‡	3	31	46	6·5
DiGeorge syndrome	14										14	29	32	43·8
Ataxia telangiectasia				1							1	8	13	7·7
Chronic mucocutaneous candidiasis					1††						1	9	13	7·7
ICF syndrome								1			1	0	1	100·0
IV. Diseases of immune dysregulation											**6**	**31**	**38**	**15·8**
IPEX syndrome		2			1					1§	4	5	6	66·7
APECED	1										1	3	4	25·0
Undetermined		1**			1**						1	2	2	50·0
V. Congenital defects of phagocyte number, function or both											**3**	**106**	**153**	**2·0**
Chronic granulomatous disease						1	1				2	54	87	2·3

Table 1. *(continued)*

PID category	Hypopara-thyroidism	Diabetes mellitus: T1D 1A	T1D 1B	Diabetes mellitus: T2D	Thyroid disease: Autoimmune hypothyroidism (Hashimoto's thyroiditis)	Thyroid disease: Non-autoimmune hypothyroidism	GHD	Hypogonadism	Isolated ACTH deficiency	Others	The number of PID patients: *n*	0–19 years	Total	Percent in total
Shwachman–Diamond syndrome							1				1	2	2	50·0
VI. Defects in innate immunity											**2**	**9**	**12**	**16·7**
NEMO deficiency										1[¶]	1	7	7	14·3
WHIM syndrome		1**				1**					1	2	3	33·3
VII. Autoinflammatory disorders											**1**	**54**	**74**	**1·4**
Familial Mediterranean fever				1[††]							1	23	36	2·8
VIII. Complement deficiencies											**0**	**18**	**23**	**0**
IX. Undetermined											**0**	**3**	**5**	**0**
Total	15	6		2	5	7	6	3	1	7	49	645	923	5·3
Estimated prevalence per 10 000 in the young population (0–19 years) of PID patients (95% CI)	232·6 (141·4–380·1)	93·0 (42·7–201·5)		15·5 (2·7–87·3)	46·5 (15·8–135·9)	108·5 (52·7–222·3)	93·0 (42·7–201·5)	46·5 (15·8–135·9)	15·5 (2·7–87·3)					
Prevalence per 10 000 in the general young Japanese population	0·072[‡‡]	1·19		0·461[§§]	30·0[§§]	13·5[¶¶]	1·47	ND	0·035					
References	[7]	[10]		[10]	[11]	[12]	[13]	ND	[14]					

SCID, severe combined immunodeficiency; ICF, immunodeficiency with centromeric instability and facial anomalies; IPEX, immune dysregulation, polyendocrinopathy, enteropathy, X-linked; APECED, autoimmune polyendocrinopathy with candidiasis and ectodermal dystrophy; NEMO, NF-κB essential modulator; WHIM, warts, hypogammaglobulinaemia, infections, and myelokathexis; T1D, type 1 diabetes; T2D, type 2 diabetes; GHD, growth hormone deficiency.

*Hypophosphatemia 1, Obesity 1.

†Obesity 2.

‡Pseudohypoaldosteronism 1.

§Adrenal crisis, Hypoglycaemia 1.

¶Hypophosphatemic rickets 1.

**Two endocrine disorders were observed in the same patient.

††the case whose onset age of a endocrine complication is 20 years or older, *n*: number of PID patients who had endocrine disorders, CI: confidence interval.

‡‡prevalence in all age groups.

§§incidence data.

¶¶prevalence in the United States, ND: no data available.

Table 2. Clinical data of T1D patients

Case		1	2	3	4	5	6
Disease		IPEX syndrome	IPEX-like syndrome	Immune dysregulation (undetermined)	WHIM syndrome	CVID	Hypogammaglobulinaemia (unknown aetiology)
Genetic mutations (gene name)		+ (*FOXP3*)	Unknown	Unknown	+ (*CXCR4*)	Unknown	NT
HSCT		–	–	–	–	–	–
Sex		M	M	F	F	F	M
Present age		8 years 5 months	14 years 5 months	21 years 8 months	18 years 9 months	19 years 1 month	25 years 3 months
Onset age of T1D		3 months	10 months	7 years 9 months	5 years 7 months	7 years 9 months	6 years 5 months
Type of T1D		1A	1A	1A	1A	1B	1B
Clinical symptoms		Polydipsia, polyuria	Polydipsia, weight loss	ND	Polydipsia, polyuria	None	None
Diabetic ketoacidosis		+ (pH 7·112)	+ (pH 7·012)	–	–	–	+ (urine ketone body (4+))
Laboratory data	Normal range						
Fasting blood glucose (mmol/l)	3·9–6·1	31·7	29·1	6·1*	7·6	8·3	7·7
HbA1c (%)	4·3–5·8	7·9	8·3	8·7*	8·9	5·6	9·1
Plasma CPR (nmol/l)	0·33–0·93	ND	0·27	0·10*	ND	0·27	ND
Urinary CPR (μg/day)	20–100	ND	ND	2·5*	15	NT	ND
Anti-GAD Ab							
Result		+	+	+*	+	None	None
Value (U/ml)	<1·5	69·1	4860	9·3*	92	ND	ND
Anti-IAA Ab							
Result		–	ND	+*	+	ND	ND
Value (nIU/ml)	<125	2·8		ND	ND		
Treatment							
Age at the start		3 months	10 months	7 years 9 months	5 years 7 months	8 years 1 month	6 years 5 months
Content		Insulin	Insulin	Insulin	Insulin	Insulin	Insulin

NT, not tested; ND, no data available; FOXP3, forkhead box P3; CXCR4, CXC chemokine receptor 4; HSCT, haematopoietic stem cell transplantation; CPR, C-peptide immunoreactivity; GAD, glutamic acid decarboxylase; IAA, insulin autoantibody.
*Post-treatment data.

some genetic factor, because the Japanese have been have reported to be one of the races with the lowest incidence of T1D.[21] With regard to the patient with WHIM, Takaya *et al.*[15] have reported that mutations of *CXCR4*, the gene responsible for WHIM syndrome, might be closely related to the development of T1D, because recent findings have suggested that impaired CXCR4 signalling is involved in the pathogenesis of T1D. The prevalence of T1D in patients with CVID was 1·1% (one in 93 patients) in our study, which was almost equal to that in the previous report.[3]

The development of T2D was observed in only one of 13 patients with ataxia telangiectasia (AT) (7·7%) in contrast to the high prevalence of T2D in the previous report (five of eight patients),[22] suggesting the unique clinical characteristics of patients with AT in Japan.

Hashimoto's thyroiditis is a relatively common endocrine manifestation in patients with IPEX syndrome.[19,20] The prevalence of Hashimoto's thyroiditis in patients with CVID in our study was 1·1% (one in 93 patients), which was similar to that of the previous report.[23] There have been only a few reports of Hashimoto's thyroiditis in patients with (S) CID.[24,25] Interestingly, this was the first report of Hashimoto's thyroiditis in a patient with CD4 deficiency, while autoimmune cytopenia is frequently associated with this disease (19%).[26] The patient with a patient with CD4 deficiency and Hashimoto's thyroiditis did not receive stem cell transplantation, suggesting that this complication was caused by autoimmunity based on the combined immunodeficiency. Nagpala *et al.*[25] reported an infant with autoimmune thyroiditis and hypothyroidism with SCID due to adenosine deaminase deficiency despite an extremely low number of T cells and a low level of IgG, which suggested that the leaky SCID phenotype permitted the survival of a few T cells with autoimmune potential.[27]

Central hypothyroidism (no TSH elevation) was observed in two patients with SCID before they received haematopoietic stem cell transplantation (Table S2), also suggesting the possibility that this complication was related to the combined immunodeficiency itself. In addition, this was the first report of primary hypothyroidism (elevated TSH levels at birth) in patients with